2021

Hydrodynamics of jet propulsion

Wright, Faye

Wright, F. (2021) 'Hydrodynamics of jet propulsion', The Plymouth Student Scientist, 14(1), pp. 452-489.
http://hdl.handle.net/10026.1/17326

The Plymouth Student Scientist
University of Plymouth

Hydrodynamics of jet propulsion

Faye Rebecca Wright

Project Advisor: Dr Jon Miles, School of Engineering, University of Plymouth, Drake Circus, Plymouth, PL4 8AA

Abstract
Water jet propulsion systems have recently developed in vessels and will continue to grow, leading to scour related problems in harbours and marinas. In order to design scour protection appropriately it is vital to understand the characteristics associated with jet flows to inform the prediction of velocities induced. The study is undertaken in two parts; a literature review of research and existing models and a physical model of a water jet propulsion system from a typical ferry. Data collection occurred along the centreline of the velocity field and in radial transects. The measurements from existing models were compared to measurements and new empirical formulae were developed to assess the accuracy of current equations. Results indicated the velocity field was symmetrical with the most turbulent flows at boundaries and in the latter stages of flow. The centreline velocity did not decay immediately, with a characteristic centreline length of 12.5D where the core region was identified. Existing velocity prediction models underpredict this core region making them less accurate when calculating jet flow. An empirical model was formed calculating the centreline and radial aspects of the velocity field. The general form of centreline flow from Albertson et. al. (1950) was followed, while a new equation radially was formed through regression analysis. In all aspects the model created generated less RMS error than existing models when compared to data collected. The study demonstrated that coastal engineers need to be aware of the characteristics and behaviour of jet propulsion systems rather than relying upon existing models to calculate safe scour protection.

Keywords: hydrodynamics, jet propulsion, water jet propulsion, scour, coastal design, flow visualisation, submerged flow, velocity profiles, COAST basin

Introduction

The purpose of this paper is to investigate the hydrodynamic flow induced by water jets and discuss the implications on scour and coastal design. In order to conduct this, research has been undertaken and data has been collected from a scaled physical model of a water jet within the COAST basin laboratory, in the University of Plymouth. Analysis of the data has been undertaken in comparison to existing prediction models.

The issue of jet velocity field prediction for scour protection design became apparent while working within industry. The design vessel for scour protection was the Superyacht 'Azzam' which is propelled by 4 hydro-jets (without the use of tugs for berthing/de-berthing). The scour protection could not be reasonably determined through the specific jet prediction formulae provided in PIANC (2015) due to lack of understanding and experience using the formula. In addition, where shallow berthing is required, as in this case, there is the most uncertainty around the effectiveness of available equations. An overly-conservative scour protection design was therefore implemented in order to ensure the design was safe in this instance due to the lack of information available around the design procedure. More research within this area will enable the level of safety within the design to be quantified so that cost effective and more sustainable provisions of scour protection can be designed.

Background

Scour

Scour is a process which occurs in the marine environment whereby waves, currents and vessel propulsion systems induce hydrodynamic shear stresses at the seabed which initiate sediment movement in the presence of a structure (Sumer & Fredsøe, 2002; U.S. Army Corps of Engineers, 2011). Scour is a threat to structural stability due to undermining of the foundations, and therefore must be considered in the design process of coastal structures to safeguard against major failure.

Harbours, marinas and berthing structures are particularly vulnerable to scour due to waves, currents and vessel induced velocities being within a confined area. This paper, however, will only consider the scour induced from water jet propulsion of vessels. While this is only one cause of scour it is arguably one of the least researched. The significance of this cause of scour is demonstrated by the case history within Hawkswood, Evans, & Hawkswood (2015). They stated that the Voyager HSS 1500 126m Stena caused 9m deep scour holes from water jets in the soft deposits of Stranraer, Scotland. Other examples of where scour damage has been caused, despite having scour protection designed and implemented is provided by Hawkswood Evans, & Hawkswood (2015). The need for more research into the hydraulics of jet propagation for engineering design is clear.

Water jet

The water jet has limited research in coastal engineering due to its recent development and introduction to the coastal environment. The first functioning commercial water jet was achieved in 1955 and only started to be implemented into vessels in 1990. In addition, the versatility of the water jet has developed to accommodate more types of vessel. Initially, only small vessels like jet skis and jet boats utilised the propulsion type however, since 2000 the demand on higher speed

and larger vessels has grown too, to include ferries, military vessels and superyachts. Increasingly, water jet propulsion systems are being chosen over propeller systems for many reasons including them having a higher propulsive efficiency, a lower vibration noise, better manoeuvrability and ability to enter shallower water as jets are positioned within the hull (unlike propellers which could snag), (Li & Li, 2013). Therefore, the design consideration of water jets in harbours and ports has only been a relatively recent development and is rapidly becoming one of the most significant sources of erosion and damage to berths (Hawkswood, Evans, & Hawkswood, 2015).

Water jets can be classified into one of the following three types: free, wall and offset jet. A free jet has no boundary, a wall jet encounters a boundary and an offset jet is formed when partially submerged (Nyantekyi-Kawakye, Clark, Tachie, Malenchak, & Muluye, 2015). In marine jet propulsion, the free or wall jet is similar to the way the jet is deflected to the seabed in berthing applications by a 'bucket' which enables manoeuvrability, this is the critical case for scour. It is evident from modelling that when the jet is deflected by a bucket the entire jet is submerged and free until the boundary of the seabed (PIANC, 2015).

A water jet propels water without the axial and radial components often found within propeller velocity flows, which produces faster velocities (Hamilton Jet, 2019). This explains the definition of a water jet within PIANC (2015) that a water jet is a modern type of propulsion system characterised by high outflow velocities of up to 25m/s. Clarity on the characteristics of induced flow and the effects on the surrounding water velocities needs to be better understood by those undertaking coastal design.

Literature Review

Review Scope

Jet hydrodynamics is not widely understood within the application of a manoeuvring vessel; therefore, the aim of this literature review is to compare previous research methods, theories and existing practical knowledge in the area. This aims to provide well-informed hypotheses upon which the study can investigate. The main sub-topics of this literature review include existing guidance, regions of flow, model theories, experimentation and visualising flow.

Scour Design Guidance

The requirement for predicting the effect ships have on berthing structures is well known and the report by PIANC (2015) is dedicated towards providing design guidance in this regard. PIANC (2015) demonstrates many methods to help design protection against scour effects of ships, it is clear that the first stage of design is to work out the induced water velocity from the vessel (which can then be converted into rock or equivalent protection). This process is more difficult than first seems and is often referred to, within the engineering industry, as a 'Dark Art'. The lack of research in the area is demonstrated by the ambiguity to which each design equation is applicable and the uncertainty between safe and economical design. Unlike other areas of coastal engineering design, where physical and numerical models can be major tools in the design process, this is not easily achieved as the physical model set up would be overly complicated and there is a lack of data available to run a numerical model. Having considered all of this, using the design methods within

PIANC (2015) is a good approach to design as it enables many specific design parameters individually to be considered together. However, in order to accurately achieve this, it is important that the equations are representative of the design situation. The extent to which propeller design formula can be used in place of specific jet predictive models will also be assessed within investigation, such as the well-established Dutch and German Methods (PIANC, 2015).

According to Hawkswood et al. (2015) the action of water jets is much more 'extreme' than that of propellers however there is not much research within this area to demonstrate the extent to which this is true or what 'extreme' action is. The prediction model specific to hydro jets presented by PIANC (2015) is the model produced by Verheij & Stolker, (2007). While the approach is endorsed within industry guidance by PIANC (2015) it has not been widely accepted and cannot be used in a lot of port project applications due to lack of accurate prediction within the jet development zone. The lack of numerical data and analysis within the paper by Verheij & Stolker (2007) makes the reliability of its predictions unclear and limits the confidence of findings within the source. The equation is included below and shown on the centreline comparative graph for completeness.

$$V_x = 12.4\, V_0 \left(\frac{A}{x}\right)^{1.17};\ V_{x,r} = V_x \exp\left(-92.75 \frac{r^2}{x^2}\right);\ (\text{Verheij \& Stolker}, 2007)$$

While the lack of water jet design guidance is known, this paper will investigate the design models currently used, their situational scope and gaps in research to date. In addition, the analysis of the velocity field from the water jet will enable empirical equations of decay to be formed.

Model Equations of Velocity Decay

Both propeller and jet flow prediction models have been considered because the development of research has overlapped. Considering both will allow assessment of the cross-applicability in the design of scour protection. All model equations found follow the same general equation forms (from Albertson et al., 1950) for established flow with only coefficients varying. Albertson et al. (1950) has been the foundational theory for the development of propeller velocity decay theory and prediction development. The theory and experimentation conducted, however, was all with relation to a plain jet and has therefore been categorised as a jet prediction model in this study.

$$V_x = (2\alpha_1)^{-1}\, V_0 \left(\frac{D}{x}\right)^{\alpha_2};\ V_{x,r} = V_x \exp\left(-\frac{1}{2{\alpha_3}^2}\frac{r^2}{x^2}\right) \qquad General\ Forms$$

All equations are for the established flow region which is defined as when $V_x < V_0$.

Table 1: Coefficients of Model Equations

Model	$\propto_1$	$\propto_2$	$\propto_3$	Comment

Albertson et al. (1950), *Plain Jet*	0.081	1	0.81	$\propto_1 = \propto_3$ for Albertson Model (made for slot outflow)
Dutch Method (PIANC, 2015), *Propeller*	0.179 to 0.25	1	0.18	$\propto_1 \approx \propto_3$
German Method (PIANC, 2015), *Propeller*	*(*Twin screw*)* 0.9 *(*Without Central Rudder) $\frac{1}{2 * 1.88 \exp\left(-0.092 \frac{h}{D}\right)}$ (With Central Rudder*)* $\frac{1}{2 * 1.88 \exp\left(-0.061 \frac{h}{D}\right)}$	*(*Twin screw*)* 0.25 (Influence of bottom and water surface only) 0.6	0.15	Only for unconfined flow
Blaauw & van de Kaa (1987), *Propeller*	0.18	1	0.18	$\alpha_1 = \alpha_3$
Crushman-Rosin (2019), *Submerged Jet*	0.1	1	0.1	$\alpha_1 = \alpha_3$
Berger et al. (1981), *Propeller*	0.488	0.6	-	Centreline equation only
Hamill (1987), *Propeller*	$\frac{1}{2 * (-11.4Ct + 6.65\beta + 2.16P')} = 0.691$	$Ct^{-0.216}\ \beta^{1.024}P'^{-1}$ =0.566	-	β =0.473 Ct=0.402 P'=1 Centreline Equation only

As seen in Table 1 there are more than twice as many models for propeller rather than jet propulsion systems, this is due to the water jets recent history.

Model Regions of Flow

In order to understand jet velocity decay and hydrodynamics it is important to define characteristic regions of flow evident. Albertson et al. (1950) recognises jet flow as having three distinctive regions of flow: the core zone where the velocity is constant; the transitional zone where velocity decay is rapid and the fully developed zone where velocity decay is slower; this is also supported by Zhou et al. (2018) and Nyantekyi-Kawakye et al. (2015). However, it has been regarded by Albertson et al. (1950) and continued research that in order to define velocity characteristics only two zones of flow require definition; a zone of establishing flow and a zone of established flow (Blaa and van de Kaa, 1978; Berger et al., 1987; PIANC, 2015). Albertson et al. (1950) identifies the boundary flow region by the beginning of turbulence at the jet axis of the flow when zone is 'established'. Albertson et al. (1950) numerically defined the distance to the start of the region (Boundary Distance) as dependent on the outflow diameter and centreline distance from the outflow, as follows: $Boundary\ Distance = 6.2D$. In addition, the zones of flow identified by Albertson et al. (1950) comprised of a symmetrical flow with two symmetrical halves (defined by a gaussian probability curve) whereby the centre is a straight line through the velocity core. This flow classification is well-supported by other research conducted (Blaa and van de Kaa, 1978; Crushman-Rosin, 2019; PIANC, 2015). This paper will analyse the flow velocities collected and knowledge gained from research of the prospective regions to establish any distinctive features of the flow, which will inform decay equation formation.

Submerged Flow Model Theories

The underlying theory behind all of the models is ensuring momentum conservation. The conservation of momentum for a propeller considers rotational momentum due to the difference in water flows. Therefore, a propeller flow field will contain more turbulence within the flow field and display a faster velocity decay than a jet. Albertson et al. (1950) undertakes the theory of the plain jet by assuming that the pressure is hydrostatically distributed throughout the jet flow; the diffusion process is dynamically similar under all conditions and the longitudinal component of velocity within the diffusion regions varies according to Gaussian normal probability. A cubic cross section of space within an expanding jet is given in Albertson et al. (1950) displaying that the net longitudinal force on the faces of the element should equal the net flux of longitudinal momentum through all faces. The validity of this theory to circular orifice outflows is uncertain. This theory is accepted by Crushman-Roisin (2019) where experimentation changes the coefficient values for the respective model produced.

Berger et al. (1981) and Hamill (1987) also accepted this underlying theory of Albertson et al. (1950), but appreciated it represented a jet flow. The propeller propulsion systems have a hub connected to the propeller by a shaft which induces rotational flow (Berger et al, 1981; Lam, Song, Raghunathan, Hamill, & Robinson, 2011). Berger et al. (1981) and Hamill (1987) recognised that the rotational flow induced by the propeller means that the maximum velocity within the water is not at the centreline of flow, like a jet, but following the rotational velocity. The model equations to this point had all assumed that the centreline of flow would contain waters of the fastest velocity, which is true for jet flow but not propellers. Therefore, calculation of efflux velocity rather than centralised velocity was used in Berger et al. (1981) and Hamill (1987) models. This enabled the worst-case velocity to be

identified for each distance from the propeller, which is more useful to design. Surprisingly, this change prediction theory for a propeller did not alter the general form of equations used. Only change in experimental constants and the removal of location specific velocity detail represented this shift in prediction.

More recently, research on propeller velocity field decay from Núñez-González, Koll, & Spitzer (2018) has supported the need for efflux velocity calculations in prediction models for propeller flow. A physical model was adapted to represent the specific characteristic of propeller flow with subject to vessels, in terms of whether a stern and rudder are present. The consistent result in all cases is that the maximum velocity of propeller flow is along the axis of rotation. However, that the velocity at axis of rotation is distorted and slower when stern and rudder effects are introduced, likely caused by the addition of turbulence from obstacles which more rapidly diffuses the outflow velocity.

With there being no identification of the location of maximum velocity for any given cross-section of flow, it is surprising that a radial model of location specific velocity prediction has been accepted. No model has amended the radial decay from that proposed by Albertson et al. (1950) which follows a gaussian decay from the jet axis. Therefore, inaccuracies of propeller radial predictions calculating efflux velocity seem probable, even when predicting the flow from a propeller. With the radial decay pattern being location specific it must be assumed that the decay occurs from the maxium velocity flow. Therefore, the propeller efflux velocity is compared to that of the jet centreline velocity in this paper.

From this research, it has been hypothesised that propeller prediction models will not be able to represent the flow presented by the water jet, even when maximum magnitudes of flow are compared.

Model Equation Experimentation

Much theory surrounds velocity decay prediction however experimentation has been the only way to parameterise differences in propeller and jet flow model equations. The methods and data analysis conducted in previous research differ and will be critically analysed below.

It might be reasonable to expect that all experiments investigating hydrodynamic aspects of submerged water jets would be undertaken in water. Surprisingly however, Albertson et al. (1950) undertook the experimentation in air, with the assumption that all low viscosity mediums, such as water, would behave in the same way. A large blower was funnelled to the rectangular outflow orifice and then the velocities within the flow field were measured. The set-up is detailed within the published research.

Conversely, Blaaw and van de Kaa (1978); Berger et al. (1981); Hamill (1987); Crushman-Roisin (2019) all undertook their physical model experiments of jet flow in water. Blaaw and van de Kaa (1978) undertook two experiments; one large and one smaller scale, modelling propeller vessel propulsion. The investigation of jet flow in this project will be undertaken within water as it is much easier to control and define currents/turbulence within the water basin than unseen currents within the air.

The physical models differed greatly between propellers and jets and the differences in method of approach. However, the consistency of the data produced which forms the same relationship between Vx, V0 and D is clear. The repeatability of the empirical relationship in the linearised plots published by Albertson et al. (1950), Blaaw and van de Kaa (1978) and Crushman-Rosin (2019). It is therefore hypothesised within this project that the general form of the centreline equation, formed by Albertson et al. (1950), is accurate.

Conversely to the centreline velocity prediction models, none of the radial models have been formed empirically. Albertson et al. (1950) assumed the longitudinal component of velocity within the diffusion regions varies according to Gaussian normal probability. This assumption has been carried forward despite very limited success of close correlation between data and the proposed relationship. Albertson et al. (1950) published this plot, conceding there is "significant scatter". This was then repeated in the work of Blaaw and van de Kaa (1978) who also conceded "rather large scatter". The research of Blaaw and van de Kaa is limited due to the lack of data analysis, and discussion of findings leads to ambiguity to the extent to which the model is valid. The scatter evident from these plots is very similar and poses a question as to whether the fundamental equation form is as accurate as possible or, as defined by Albertson et al. (1950), just a "good approximation". The use of the normal error curve for the radial model can be justified as it provides a convenient determination of the equation. It appears, however, to be at the risk of inducing significant error to velocity prediction. Within this project an empirical equation will be formed from the measured data to compare it to the existing form of the current models. It is hypothesised that the existing general form of the radial decay model is inaccurate.

As seen in Table 1 the coefficients associated to the prediction models differ greatly. Differences in coefficient may be due to differences in variables within the experiments undertaken; leading to an ambiguity whether the cause is refining of the model equation itself or adjustment to other variables. Variables such as the shape of orifice, experimental approach and type of propulsion are all anticipated to have an effect. Therefore, direct comparison between the models becomes difficult.

Consequently, in industry, the difficulty in identifying the most accurate design model for water jet propulsion is evident. This project aims to present the similarities and differences of different models and compare them to water jet velocity data collected.

All experiments will undergo specific issues relating to set up and collection of data which impedes upon ability to collect accurate results or reduces ability to collect data efficiently. According to Albertson et al. (1950) the largest experimental issue was that of measuring the flow within the zone of established flow which was iterated by Blaaw and van de Kaa (1978). This stated that there was difficulty in determining accurate velocity at the areas of turbulence which create large deviation in readings, and turbulence is particularly prevalent within the zone of established flow and at the boundaries between ambient fluid and jet flow.

With turbulence playing such a large role in the anticipated experimental error of models created to date, this project aimed to define the turbulent characteristics of flow and use data logging to ensure large volumes of velocity data can average to

remove the large deviations anticipated. Problems in preliminary experimentation prevented data logging being utilised in this project.

Flow visualisation

Visualisation of flow fields has been a fundamental part of understanding the water jet decay since researched into submerged jets began. Albertson et al. (1950) discharged smoke from the orifice in order to visualise the flow and make data collection easier. More recently, Crushman-Roisin (2019) also used the visualisation of the jet flow, using dye, to define a characteristic diffusion angle of the jet. A consistent conical shape was revealed. In addition, it enabled the diagram of jet flow to be amended from that previously accepted by Albertson et al. (1950).

Forms of numerical modelling, like CFD, have often been performed in this type of investigation. However, it is conceded by PIANC (2015) that the models produced are very difficult to validate due to the experimental measurement being difficult to execute. Observational data will be used in this project in order to better understand the flow present in a water jet and validate equations created. Preliminary experiments implementing dye into the flow had limited success. Therefore, velocity contour plots and 3D plots will be produced from the data to visualise the jet flow.

Summary

The literature review has enabled the studies aims, objectives and expectations to be established. The paper aims to analyse flow velocities in a physical model, with the collection of both numerical and observational data, to inform upon the characteristics of the velocity field. Turbulence within the basin will be carefully controlled and turbulent flow characteristics, induced by the jet, will be noted. Empirical relationships for the prediction of water velocities in locations surrounding the water jet will be formed. These aims will help to collect data which can test the hypotheses formed from the evaluation of existing research above. The propeller prediction models are hypothesised to be inaccurate in representing the flow produced by the water jet. The centreline general form used, originally from Albertson et al. (1950), is hypothesised to accurately represent jet velocity flow. However, the radial general form used is hypothesised to not be the most accurate relationship for predicting jet velocity flow.

Methodology

The COAST Basin

Physical model experiments were carried out in the Plymouth University COAST basin, which is 15.5 meters long, 10 m wide and 0.5 m deep.

Pre-existing I-beams running across the width of the basin at internal distance 4m apart allowed girders to be secured with clamps. This defined a framework around the data collection zone. In addition, the framework enabled data collected to be associated to an accurate location in relation to the outflow. The basin being much larger than the data collection area allowed the dissipation of jet energy to prevent more complex flows being created by the model effects of the side walls (Zhou,

Zhang, Li, & Xu, 2018). The dimensions of basin components are indicated in Figure 1.

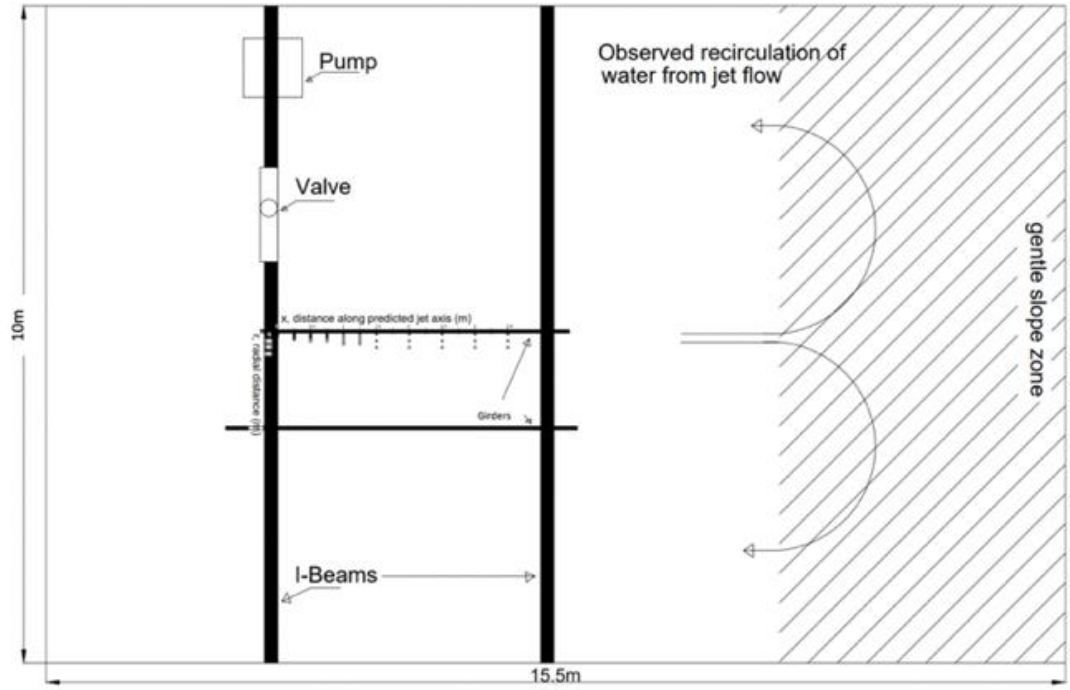

Figure 1: Diagram of plan view COAST basin set-up

A Draper water pump, stock number 69690 with discharge 320litres/min and maximum head of 11m, was attached to pipework where the outflow is a physical model of a jet propulsion system. The pipework consists of both flexible plastic and solid copper pipe with a valve installed between the pump and outflow, above the water surface, to ensure velocity at the outflow was consistent throughout as seen in Figure 2 and Figure 3. The water pump was secured to two scaffold poles which were drilled into the basin floor and tied down to prevent any kickback that could dislodge any of the pipes. The individual pipes were circular, the copper outflow with a diameter of 0.026m and 0.2m in length.

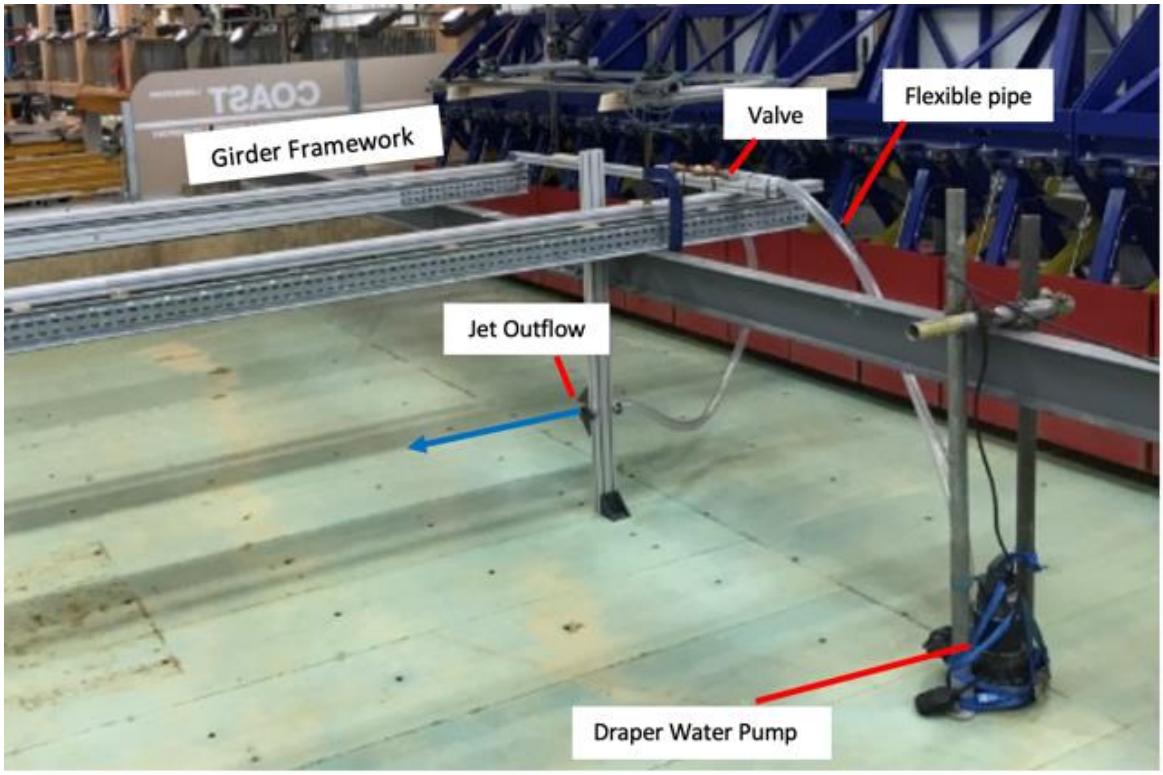

Figure 2: Photograph of set-up of water pump, pipework, valve and outflow in empty basin

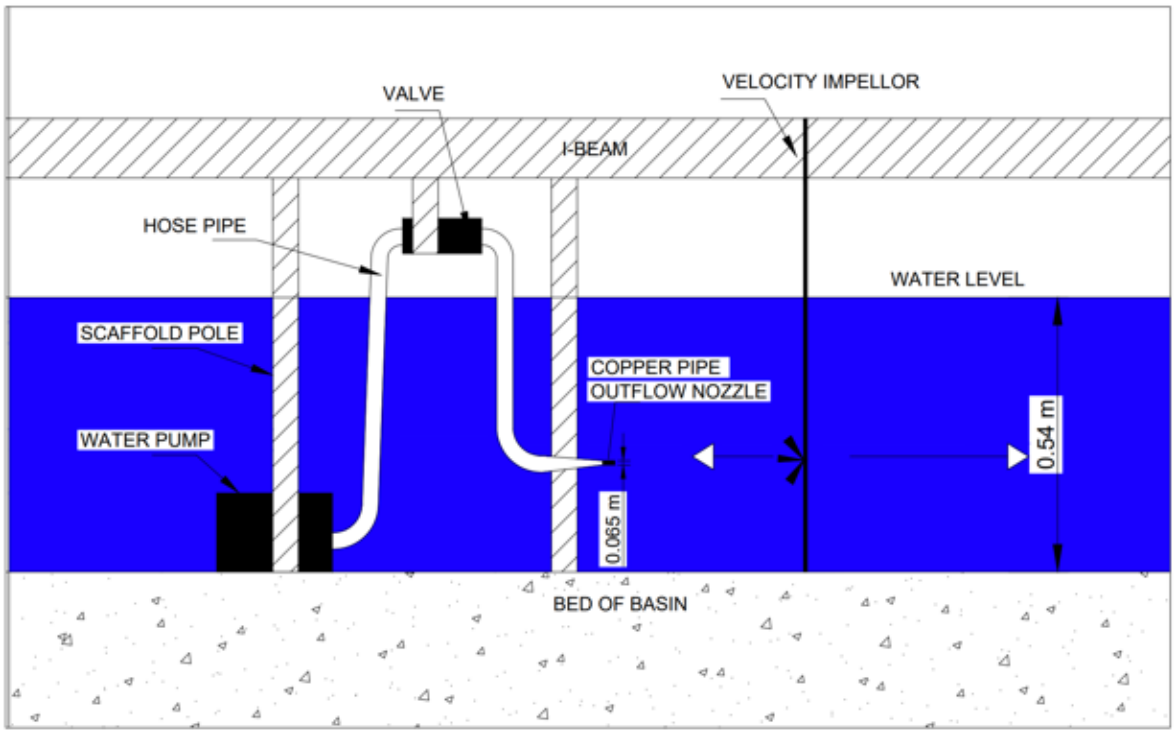

Figure 3: Diagram of Experiment Set Up

Significant head losses occurred from the pump to the pipe exit because of friction, bends in the pipe, change in pipe diameter and exit loss. This reduced the largest outflow velocity possible to just under 2m/s. The valve was not needed to reduce the

velocity to the scaled outflow velocity as presented in the following section. The volume of pipework used was primarily to ensure that the water jet was as far away from the jet outflow as possible in order to prevent distortion in data collected.

Figure 4: Photo of Data Collection with Velocity Impellor

The basin held still water in order to solely measure the hydrodynamic impact imposed by the water jet physical model. Measurements were taken with the Valeport 'Braystoke' Model 001 flow meter (Valeport, 2020). The 8011 series high impact Streyrene Impellor head was chosen sized at 125mm diameter with 270mm pitch. The range of flow measurements was between 0.3m/s and 10m/s which is within the anticipated range. The impellor also had a higher accuracy than that of smaller impellor heads, at +/- 1.5% of readings above 1.5m/s. The velocity impellor was calibrated with "Group Calibration" according to BS ISO 2537:2007 (Valeport, 2020). The impellor was positioned securely against the framework at each location, centrally and radially, and was held to the bed of the basin, see Figure 4Figure 3. The adjustable height of the impellor allowed the impellor to be 0.27m from the bed of the basin for central and radial measurements and adjusted as necessary for the depth profile.

Velocities were displayed on the real-time control unit. Data was collected manually from real-time every 5 seconds, with 10 readings at each location. The velocities collected were averaged which minimised the impact of turbulence as the velocity would fluctuate as eddies passed. The data collection points are displayed in Figure 5, location of data points was optimised to give a high resolution on the region near the jet, with reduced resolution further from the jet.

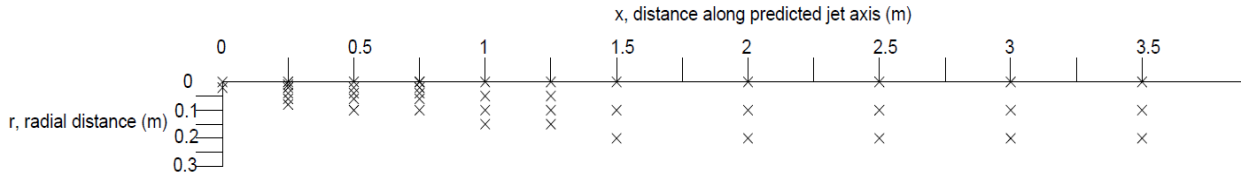

Figure 5: Data Collection Points in relation to Jet Outflow (0,0)

Prototype Field Parameters

In order to accurately convey a water jet propulsion system in a physical model, a representative prototype water jet was made. It is clear that every type of vessel is likely to have some fluctuation in the flow field created. Since ferries have characterised previous research into the water jets, this protype was based on available typical ferry information and the Solano Ferry. Typical ferries, according to PIANC (2015), have cruising jet velocities of 19m/s with manoeuvring velocities around 13m/s which is also in line with the speed characteristics of the Solano Ferry. Therefore, the prototype jet exit velocity, V_0, is set at 13m/s. The prototype pipe diameter is 1.12 m, based on the average hydro jet outflow opening area being $1m^2$ (PIANC, 2015).

Model Scaling

Jet velocity field length before total decay was anticipated to not be greater than 150m in length. In order to ensure dissipation in the basin and minimise the reflection and distortion of data, data was collected over a length of 3.5m which enabled a geometric scaling of 1:43 possible. Velocity was scaled according to Froude similitude as detailed in Hamill (2011). Pragmatic choice of pipe size, of 0.0262m, was made in order to meet standard sizes to enable sourcing of the pipe for the experiment possible, while still following the diameter geometric scaling of 1:43. All scaled parameters are acknowledged in Table 2.

Reynold's scaling was briefly considered due to the turbulence of flow being a significant characteristic of jet flow. However, it was deemed unreasonable and unfeasible to drastically increase velocity for reduction in diameter size to conserve turbulence, as the characteristics of turbulence are not documented well enough to enable accurate conservation through the Reynold's number.

Table 2: Parameters Guiding the Experiment

Parameter	Scaling (1:43)	Prototype	Model
Jet Outflow Diameter, *D (m)*	S	1.12	0.026
Exit Velocity, *V_0 (m/s)*	$S^{0.5}$	13	2
Length of Velocity Field, x (m)	S	150	3.5

Results and Data Analysis

Data was collected in order to investigate hydrodynamic characteristics and define a unifying relationship to describe the distribution of collected velocity data over the entire domain. This also allowed comparison with other predictive models.

Velocity Decay along the jet axis

The data collected along the centreline of the jet flow was averaged. These velocity values are plotted against centreline distance in Figure 6.

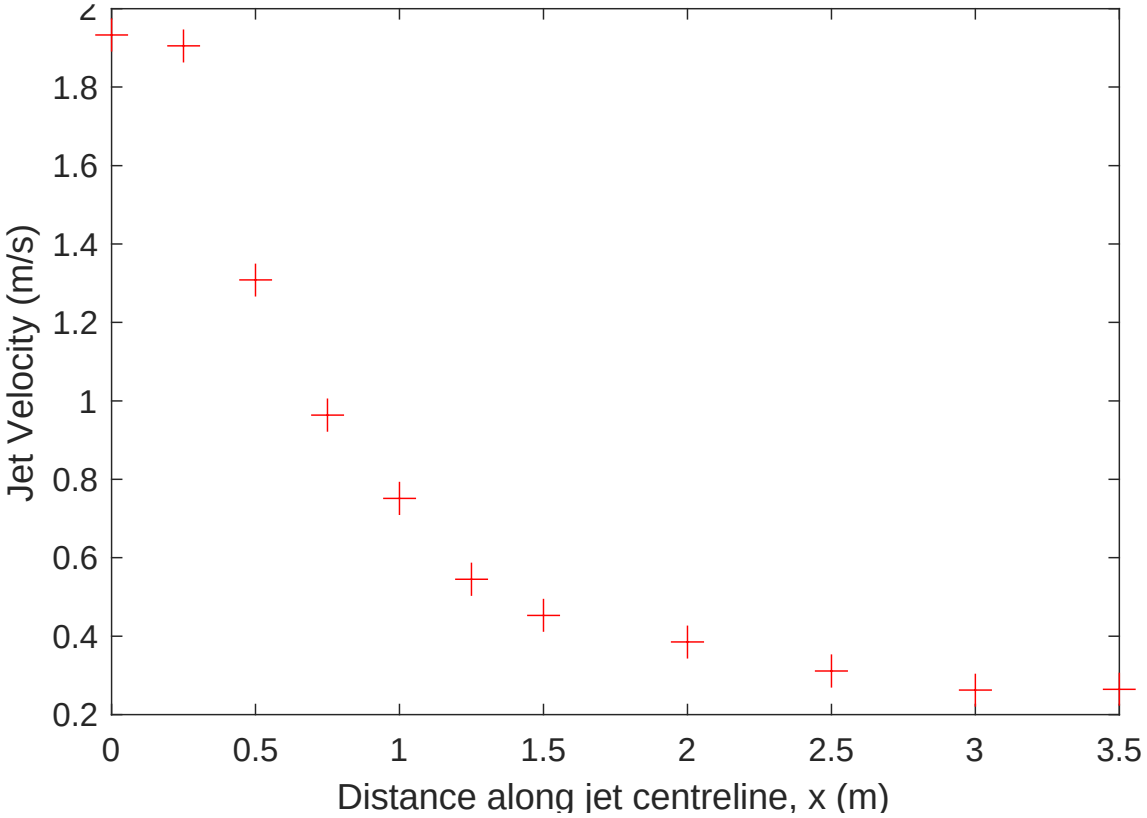

Figure 6: Averaged Jet Velocity Data against Centreline distance

Measurements of the centreline velocity from the experiment were plotted as a dimensionless logarithmic plot in Figure 7. Close to the outflow $V_x / V_0 = 1$ demonstrates the core region. A linear trend is formed presenting the established flow region which defines the centreline empirical relationship in Equation 1. Equation 1 explains 98.96% of the data variation for centreline velocity which is given below:

$$V_x = 10\, V_0 \left(\frac{D}{x}\right)^{0.906} \quad [Equation\ 1]$$

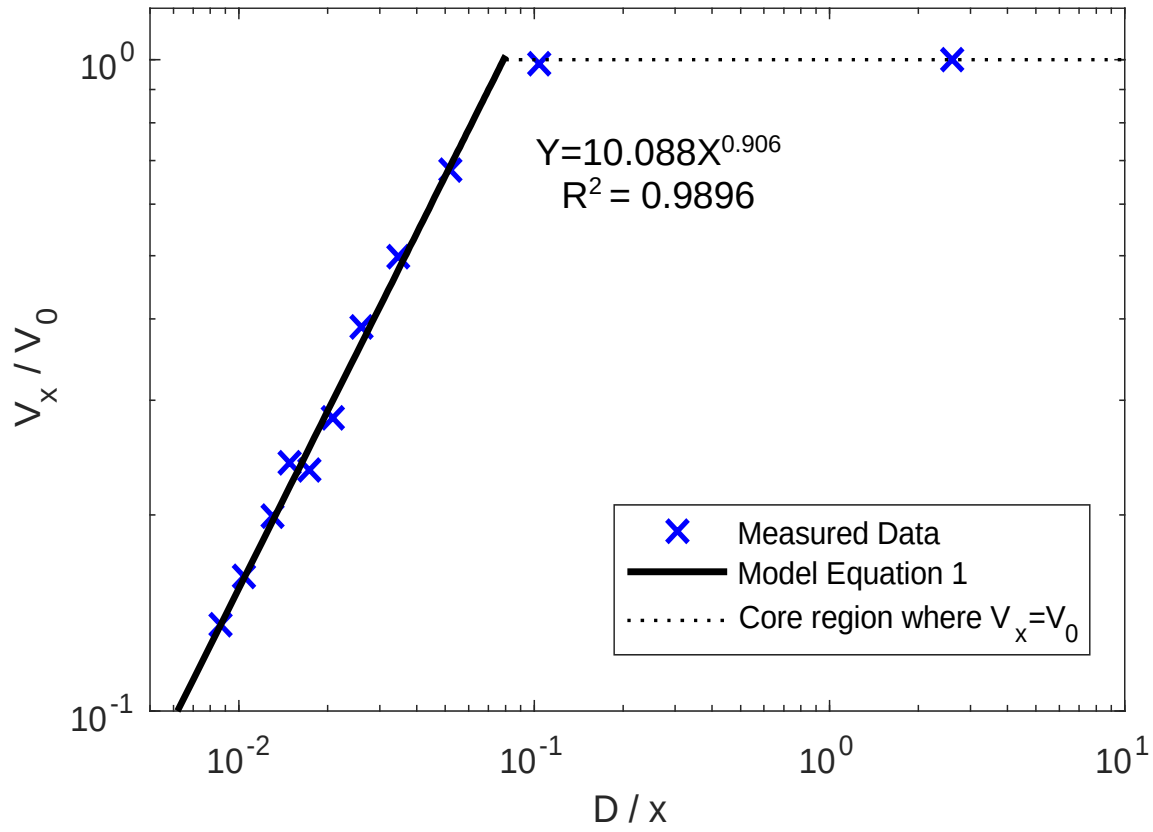

Figure 7: Dimensionless logarithmic plot of collected centreline velocity

A Pearson's Product Moment Correlation Coefficient (PPMC), denoted by r_C, was calculated for the linearised centreline relationship showing an almost perfect negative correlation between log(x/D) and log(V_x/V_0).

$$r_C = \left(\frac{\sum_{i=1}^{n} x_i y_i - \frac{\left(\sum_{i=1}^{n} x_i\right)\left(\sum_{i=1}^{n} y_i\right)}{n}}{\left(\left(\sum_{i=1}^{n} {x_i}^2 - \frac{\left(\sum_{i=1}^{n} x_i\right)^2}{n}\right)\left(\sum_{i=1}^{n} {y_i}^2 - \frac{\left(\sum_{i=1}^{n} y_i\right)^2}{n}\right)\right)^{0.5}}\right) = -0.995$$

The mean of the residuals from the centreline jet velocity decay model is -0.0049, and a plot of the residuals is given in Figure 8.

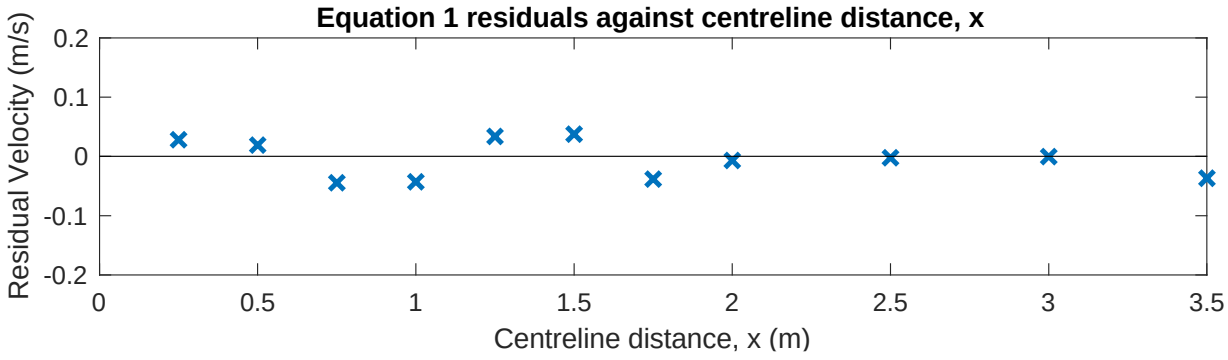

Figure 8: Plot of residual centreline velocities from model Equation 1

The existing models are plotted along with data collected and Equation 1 for comparison in Figure 9.

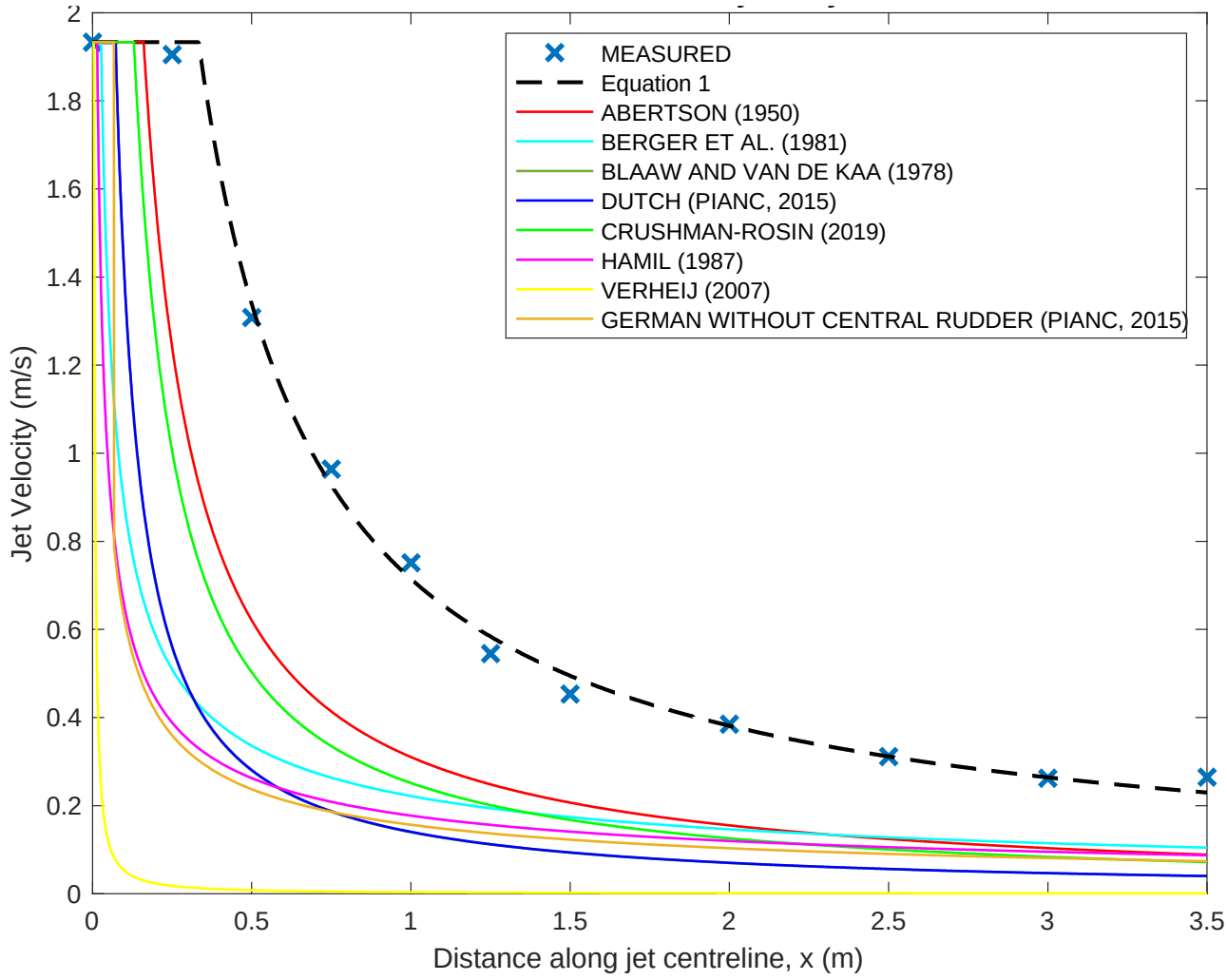

Figure 9: Centreline Jet Velocity Decay compared against models

A Root-Mean Squared (RMS) Analysis was carried out as a measure of error around the model equation and the existing models. A table detailing the numerical ranked order RMS error for the centreline of the velocity decay models can be found in Table 3.

$$RMS\ Error = \sqrt{\frac{1}{n}\sum((V_{measured} - V_{model})^2)}$$

Table 3: Centreline RMS Error for all models against collected data

Type of Propulsion	Model	RMS Error
Jet	Equation 1	0.0284
Jet	Albertson et al. (1950)	0.3935
Jet	Crushman-Roisin (2019)	0.4752
Propeller	Berger et al. (1981)	0.6032
Propeller	Hamill (1987)	0.6546
Propeller	Dutch Method (PIANC, 2015)	0.6335-0.6912
Propeller	Blaauw and van de Kaa (1987)	0.6349
Propeller	German Method (PIANC, 2015)	0.6720

Velocity Decay along the jet axis

The measured velocity of the jet against radial distance is presented in FIGURE. It is clear that centreline distance from the jet influences the radial velocity anticipated at a given location.

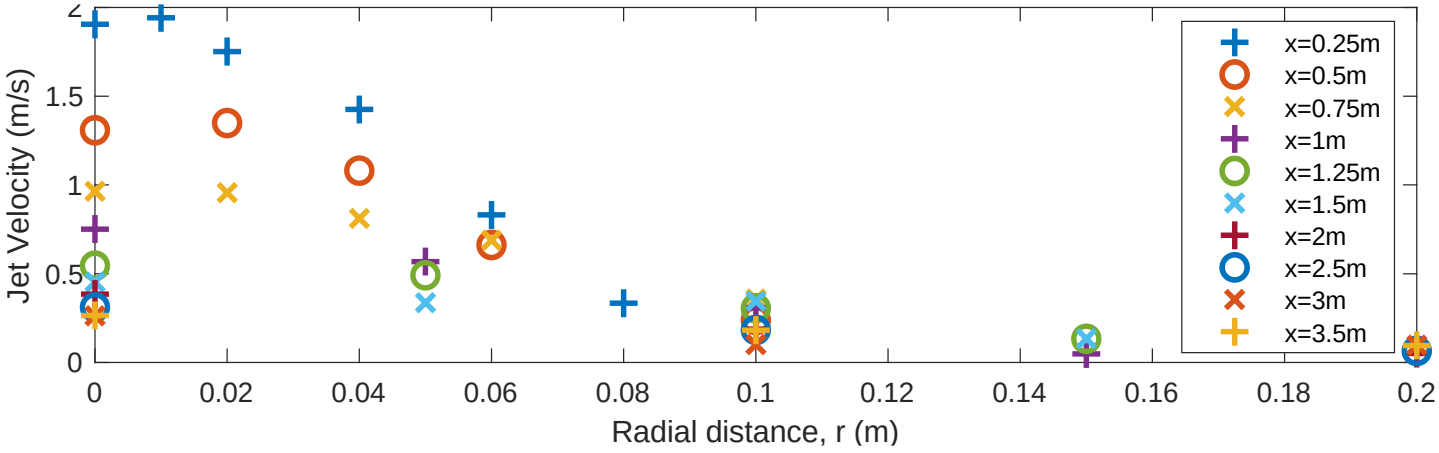

Figure 10: Average Jet Velocity with respect to radial distance

Regression analysis for the radial data (and all values of x) was implemented in order to find a linearised best fit of the data as shown Figure 11. This formed the equation below:

$$V_{x,r} = V_x \exp\left(-86.73\frac{r^2}{x}\right) \; [Equation\ 2.1]$$

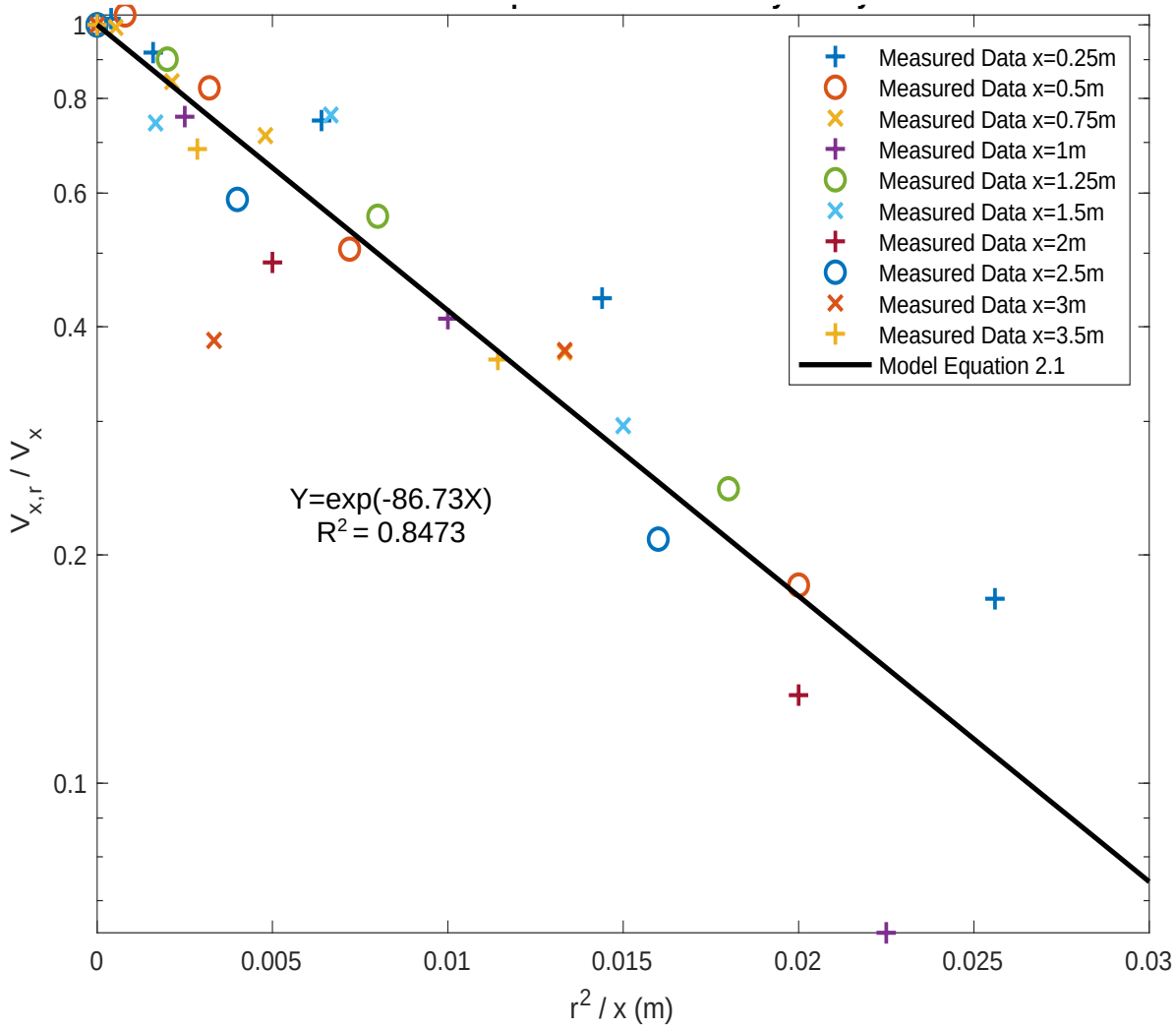

Figure 11: Average Jet Velocity with respect to radial distance

A Pearson's Product Moment Correlation Coefficient, denoted by r_C, was calculated from the linearised radial relationship. The result indicates an strong negative correlation between log(x/D) and log($V_{x,r}/V_x$).

$$r_C = \frac{\sum_{i=1}^{n} x_i y_i - \frac{(\sum_{i=1}^{n} x_i)(\sum_{i=1}^{n} y_i)}{n})}{\left(\left(\sum_{i=1}^{n} {x_i}^2 - \frac{\left(\sum_{i=1}^{n} x_i\right)^2}{n}\right)\left(\sum_{i=1}^{n} {y_i}^2 - \frac{\left(\sum_{i=1}^{n} y_i\right)^2}{n}\right)\right)^{0.5}} = -0.915$$

The mean of the residuals from the radial jet velocity decay model is -0.08355, and a plot of the residuals is given in Figure 12. The variance of data is larger when x<1m therefore an empirical relationship for this zone of flow was made.

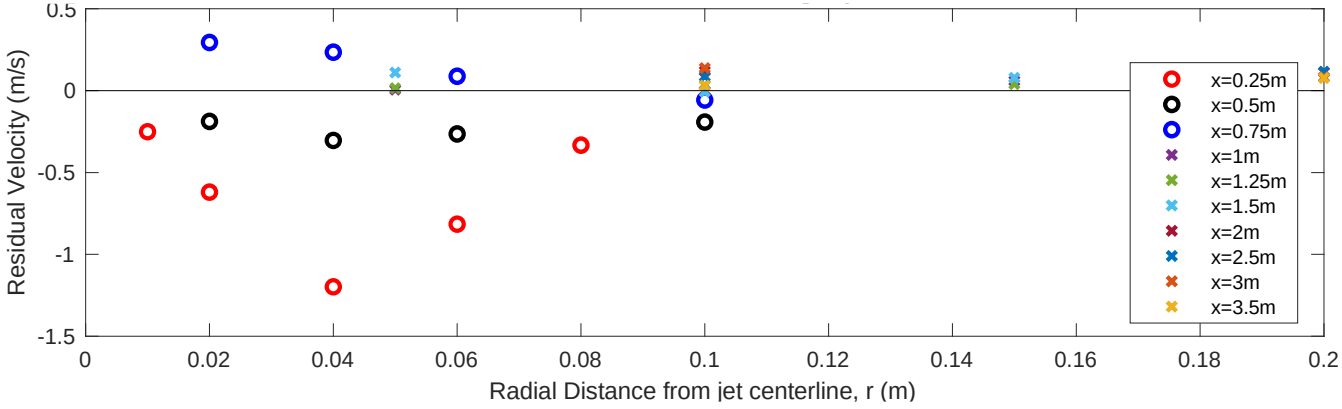

Figure 12: Plot of Residual Radial Velocities from Equation 2.1

When the data for x<1m was looked at individually it enabled Equation 2.2, explaining 95.83% of the data, to be formed for axial velocity, see Figure 13.

$$V_{x,r} = V_x \exp\left(-71.94\frac{r^2}{x}\right) [Equation\ 2.2]$$

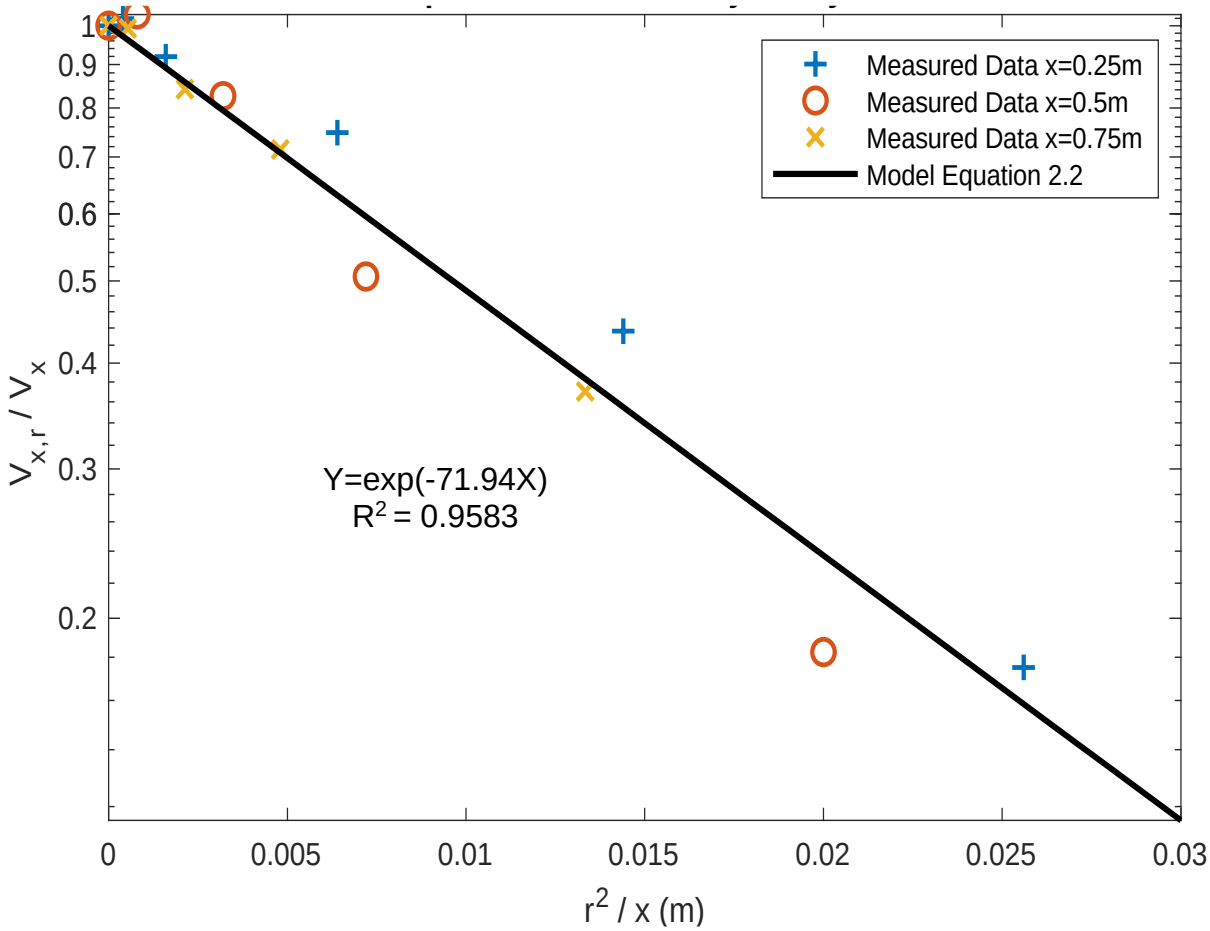

Figure 13: Radial trend linearised for x<1m of data collected

A Pearson's Product Moment Correlation Coefficient, denoted by r_C, was calculated from the linearised radial relationship for x < 1 m. The result indicates an strong negative correlation between log(x/D) and log($V_{x,r}/V_x$).

$$r_C = \frac{\sum_{i=1}^{n} x_i y_i - \frac{(\sum_{i=1}^{n} x_i)(\sum_{i=1}^{n} y_i)}{n})}{\left(\left(\sum_{i=1}^{n} {x_i}^2 - \frac{\left(\sum_{i=1}^{n} x_i\right)^2}{n}\right)\left(\sum_{i=1}^{n} {y_i}^2 - \frac{\left(\sum_{i=1}^{n} y_i\right)^2}{n}\right)\right)^{0.5}} = -0.945$$

A plot of comparison of the distribution of the residuals given in the first meter of jet flow of Equation 2.1 and 2.2 is given in Figure 14.

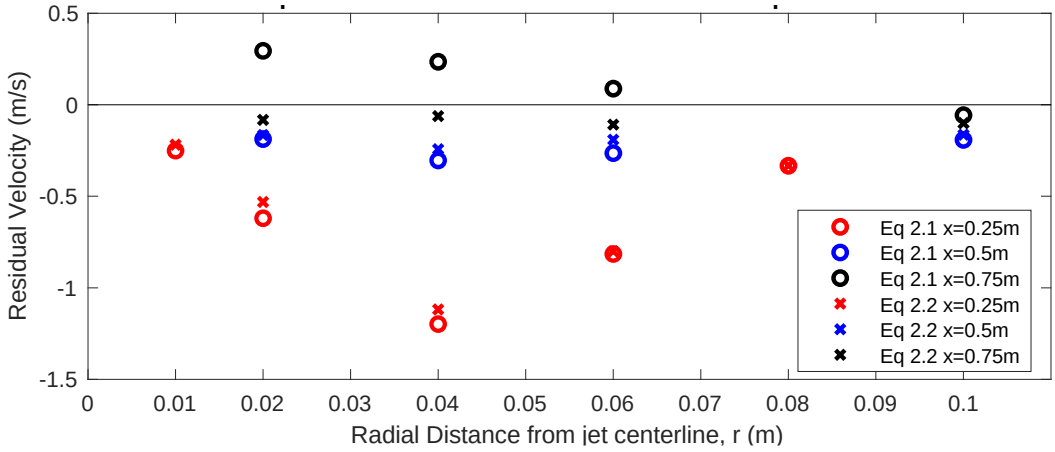

Figure 14: Comparison of the residuals resulting from Equation 2.1 and 2.2

A Root-Mean Squared (RMS) Analysis was carried out as a measure of error around the radial model equations and the existing models. RMS analysis for each radial model has been conducted and tabulated below.

Table 4: Radial RMS Error for all models against collected data

Type of Propulsion	Model	RMS Error
Jet	Equation 1 along centreline; Radially, Equation 2.1 when x<1m and Equation 2.2 x≥1m	0.0598
Jet	Equation 1 along centreline; Radially, Equation 2.1 only	0.820
Jet	Albertson et al. (1950)	0.4417
Jet	Crushman-Roisin (2019)	0.4621
Propeller	Blaauw & van de Kaa (1987)	0.5477
Propeller	Dutch Method (PIANC, 2015)	0.5708
Propeller	German Method (PIANC, 2015)	0.6212

In addition, the RMS Error is presented in Figure 15 to detail how the radial error of each model changes with distance from the outflow. Equation 2.1 is presented for all values of x, and Equation 2.2 is presented for x<1m.

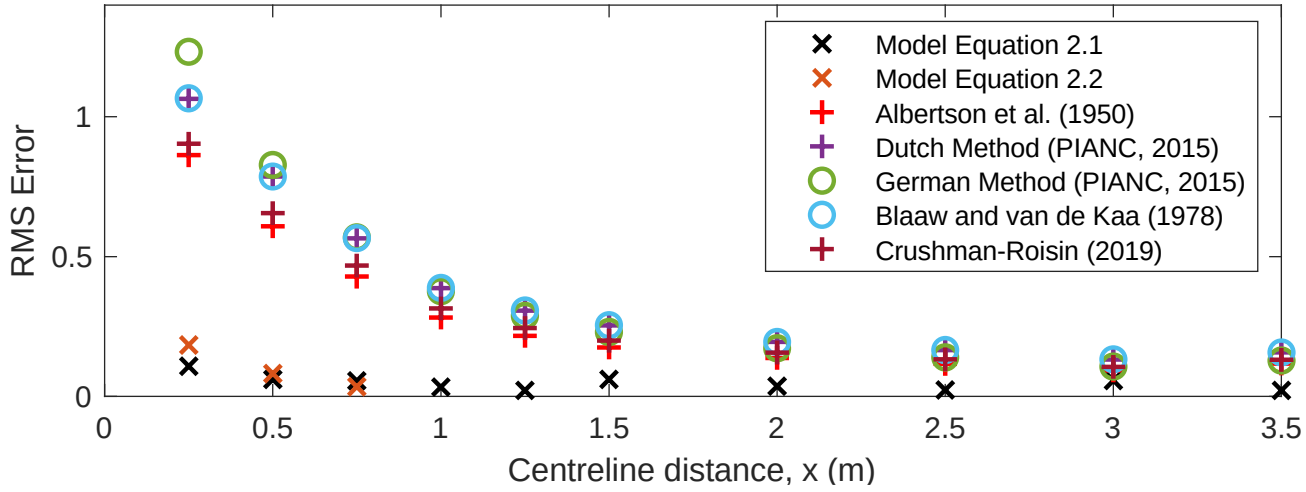

Figure 15: Comparative Radial RMS Error with respect to Centreline

Individual radial transect graphs are presented from Figure 16 to Figure 25. Measured average velocity is plotted against respective model equations for comparison. Equation 2.1 is presented on all transects, and Equation 2.2 is presented on transects where x<1m according to the data set each empirical equation was formed from.

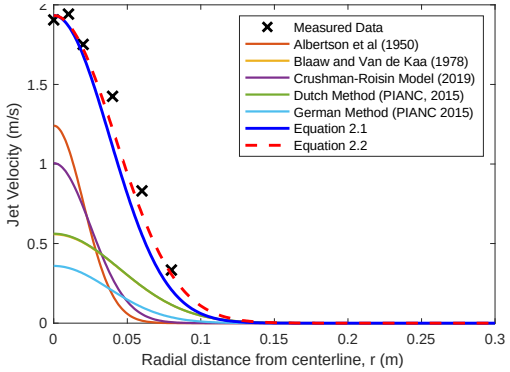

Figure 16: Comparative radial velocity decay graph at x=0.25m

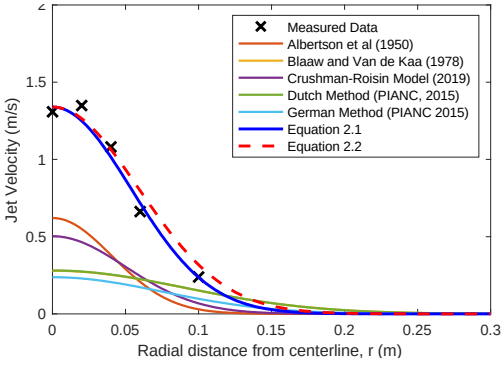

Figure 17: Comparative radial velocity decay graph at x=0.5m

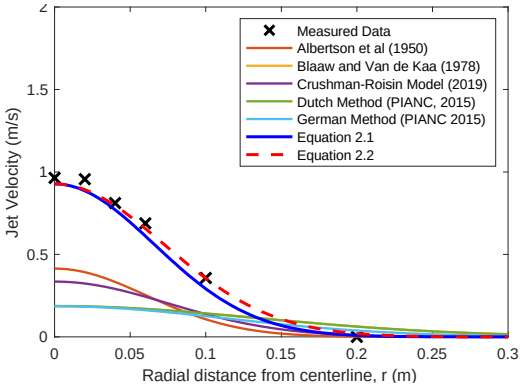

Figure 18: Comparative radial velocity decay graph at x=0.75m

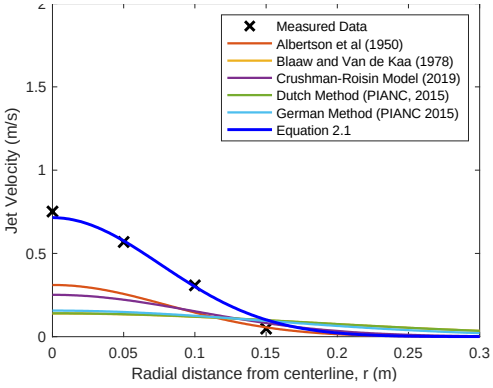

Figure 19: Comparative radial velocity decay graph at x=1m

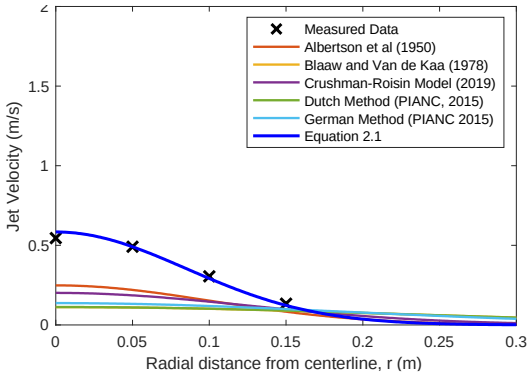

Figure 20: Comparative radial velocity decay graph at x=1.25m

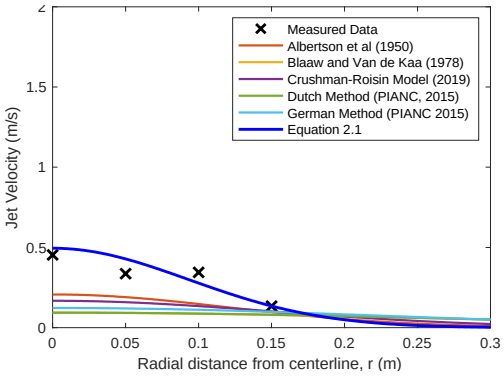

Figure 21: Comparative radial velocity decay graph at x=1.5m

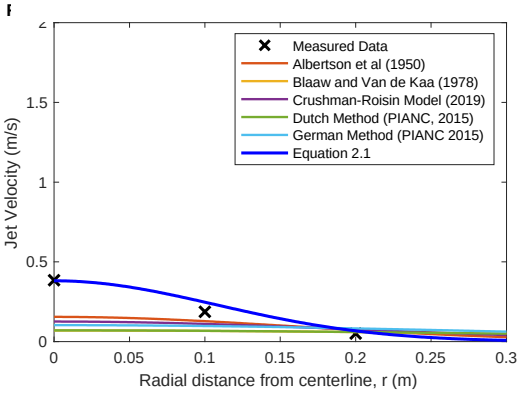

Figure 22: Comparative radial velocity decay graph at x=2m

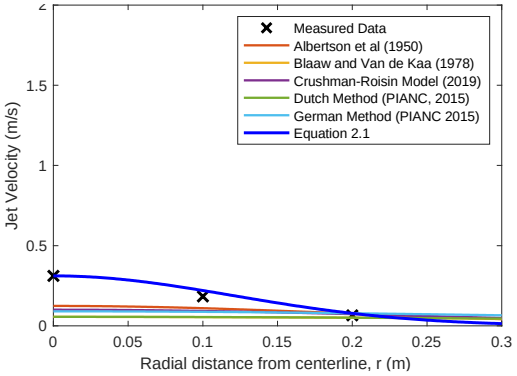

Figure 23: Comparative radial velocity decay graph at x=2.5m

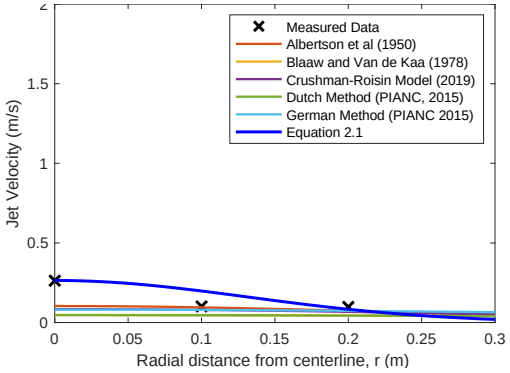

Figure 24: Comparative radial velocity decay graph at x=3m

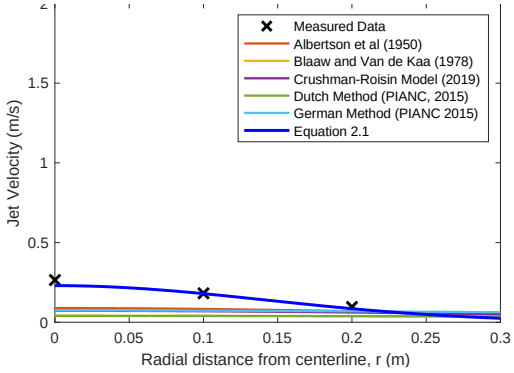

Figure 25: Comparative radial velocity decay graph at x=3.5m

Velocity Profiles

The velocity contour map in Figure 26 displays the data collection points which are mirrored to form the plot. The respective equations formed the contour plot (Equation 1 at the centreline, and Equations 2.1, 2.2 radially when $x \geq 1$m and $x < 1$m respectively), seen in Figure 27.

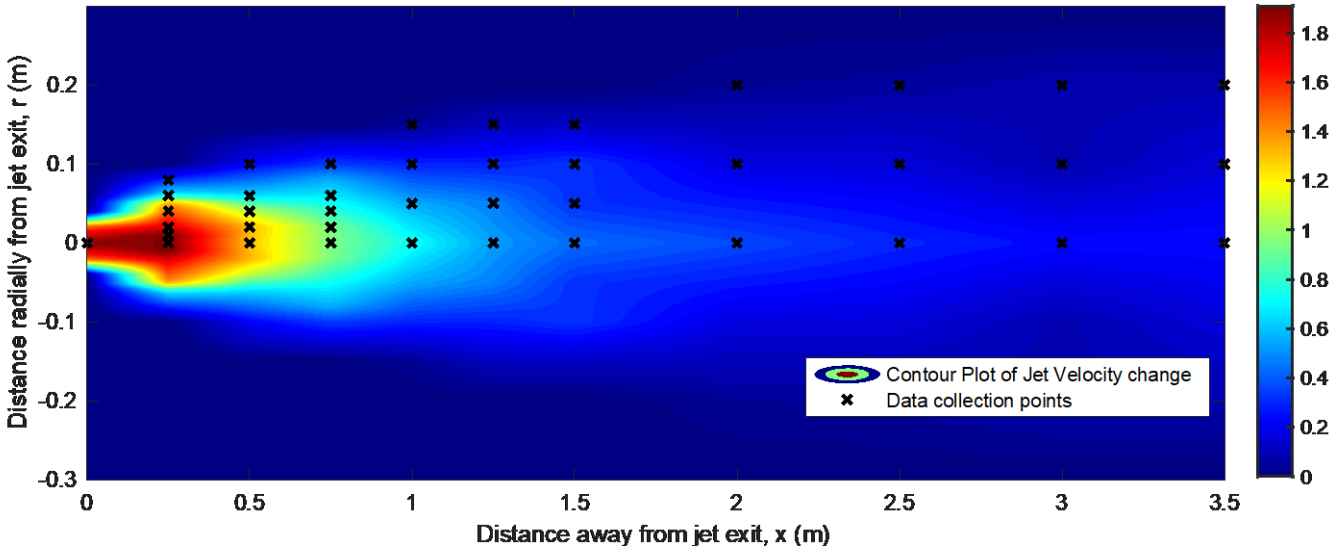

Figure 26: Measured Jet velocity Decay Contour Graph with data collection points mirrored onto the other half of the jet.

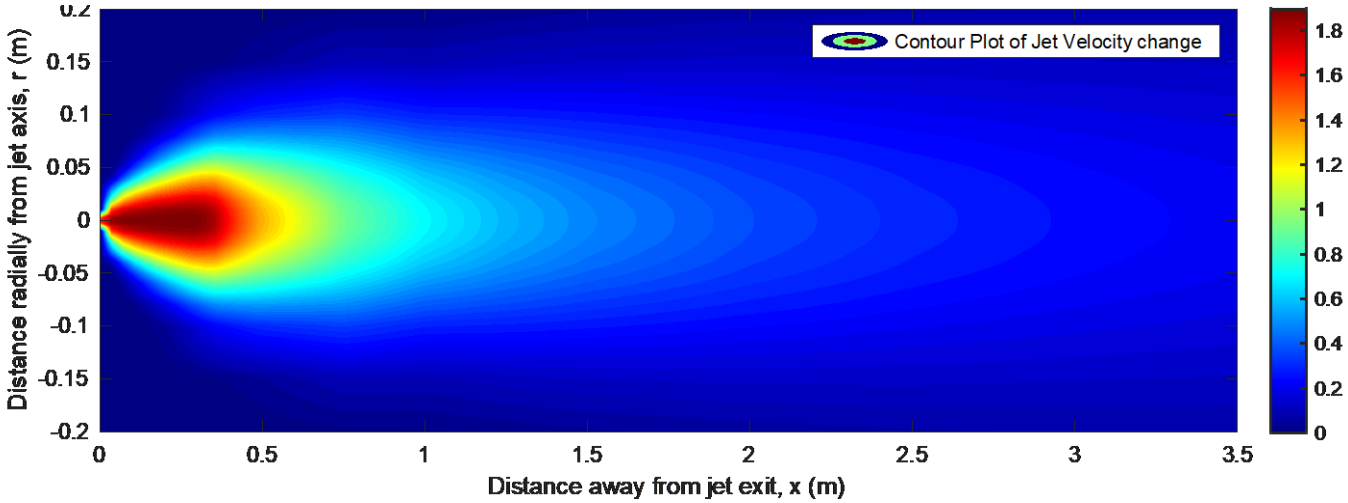

Figure 27: Jet Velocity decay graph made from empirical equations (Equation 1 at centreline, Equation 2.1 when x<1m and Equation 2.2 radially when x ≥ 1m)

The depth velocity profile from mirrored data collected is presented in Figure 28 with proportionally scaled axes and the data collection point locations on the plot. Figure 29 is the predicted cross-section at x=1m according to Equation 2.1.

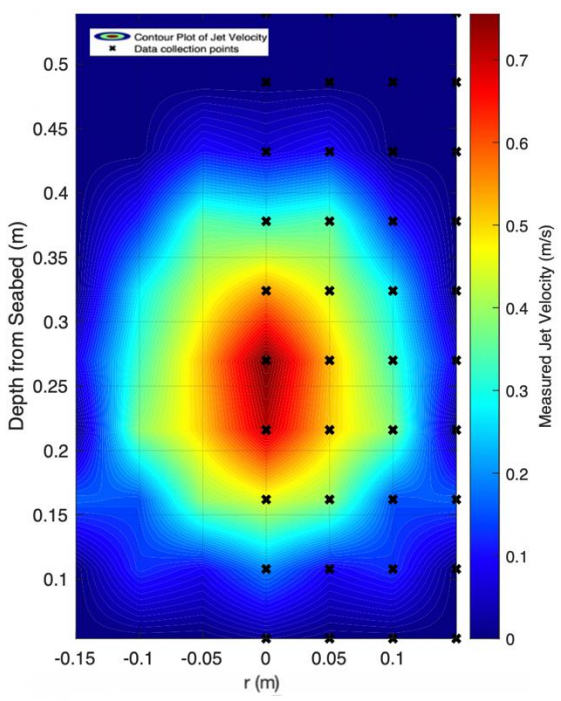

Figure 28: Contour Plot of velocity throughout the depth of 1m transect

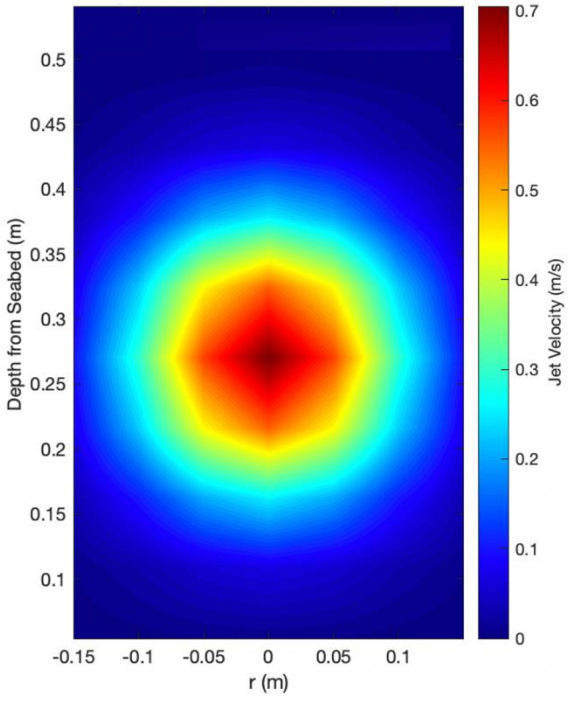

Figure 29: Contour Plot of the predicted velocity at x = 1m according to Equation 2.1

The cross section profile data has also enabled a 3D plot of the velocity to be produced and compared in several orientations to Equation 2.1 in Figure 30 to Figure 35.

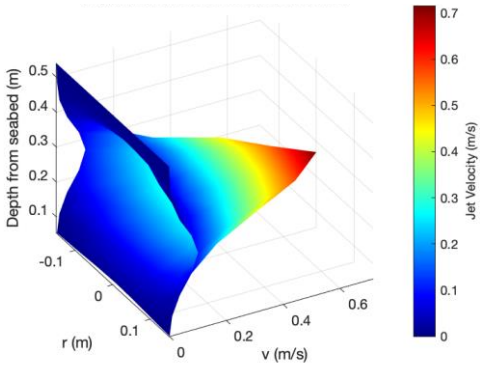

Figure 30: Orientation 1: 3D Plot of velocity cross-section at x=1m from Equation 2.1

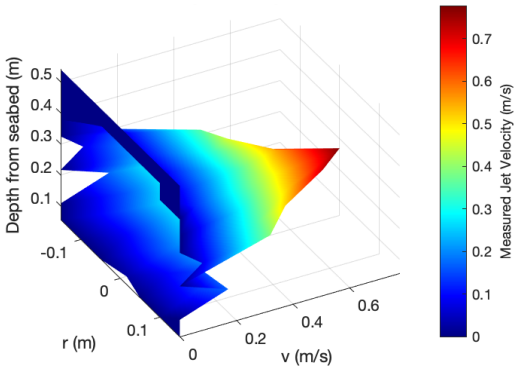

Figure 31: Orientation 1: 3D Plot of measured velocity at x=1m

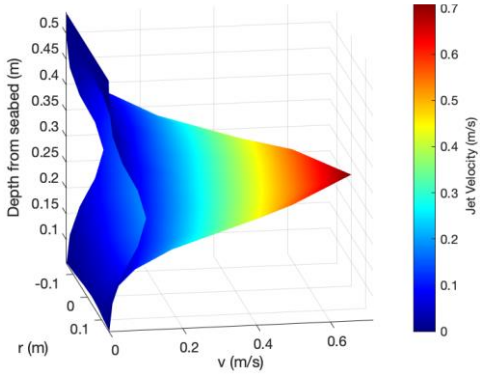

Figure 32: Orientation 2: 3D Plot of velocity cross-section at x=1m from Equation 2.1

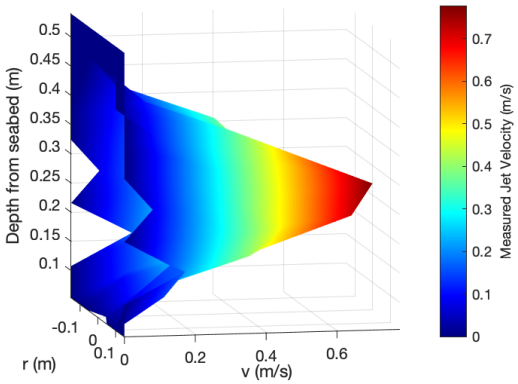

Figure 33: Orientation 2: 3D Plot of measured velocity at x=1m

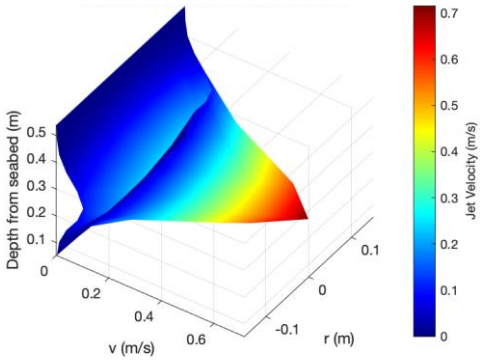

Figure 34: Orientation 3: 3D Plot of velocity cross-section at x=1m from Equation 2.1

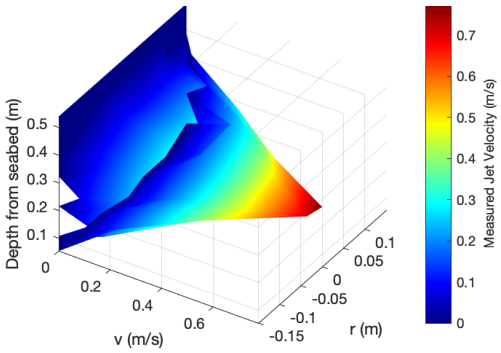

Figure 35: Orientation 3: 3D Plot of measured velocity at x=1m

Results Discussion

Data is discussed in this section, with regards to findings of velocity field characteristics in line with one of the project's aims.

Maximum jet velocity decay and cross-section profile of velocity field

The velocity field was produced by a jet of water through a symmetrical circular orifice. The resulting velocity field is characterised by the circular cross profile where the maximum velocity, for any given value of x, is located at the jet centreline as evidenced in Figure 28. These findings support the previous research on cross profile characteristics of water jets. A slight vertical elongation of the flow is evident in the cross profile presented in Figure 28, which differs to that of the circular pipe outflow shape. It can be inferred from this that a source of error is present, but the cause is ambiguous.

As previously shown in Figure 1, the horizontal recirculation pattern within the basin which was observationally evident may have disrupted the horizontal velocities of the jet more than the vertical velocities. Since all radial measurements were taken in the horizontal aspect of the velocity field, the radial decay empirical models may not be representative of undisrupted flow. In Figure 29, Equation 2.1 is used to show a cross section prediction of symmetrical circular velocity. The radial decay of the jet from the centreline is very similar to the horizontal aspect of Figure 28, but with faster decay in the vertical plane.

Another potential source of the elongation presented in Figure 29, could be that the copper pipe was secured with, or was not secured enough to prevent, a vertical tilt. The visible elongation at x=1m would be evidence that the cross profile of the flow was not parallel to the jet outflow. Experimental difficulty was found when setting up the pipe network connected to the pump; therefore, it is possible that the pipe could have moved. In this case the horizontal plane of the jet would hold the least error for radial velocity measurement at a controlled centreline distance. Therefore, Figure 29 would be a more accurate presentation than Figure 28, of how the jet flow cross profile is characterised, due to it presenting the cross profile as parallel to the outflow.

Alternatively, the jet axis location may not have been correctly identified and therefore the elongation is a presentation of the data gap. However, this is considered unlikely due the presentation of a clear core region of flow along the centreline identified, as presented in Figure 7.

In addition, the 3-Dimensional presentation of measured velocities, in Figure 31, Figure 33 and Figure 35 present a largely consistent conical shape which are conducive with anticipated results following the work of Crushman-Roisin (2019). The small discrepancies, evident from bumps on the surface, may be caused by turbulence which has not totally been removed from averaging readings collected. It was previously detailed, that there was a need to limit the contact of the jet flow within the model boundaries. While no velocity distortions at the bed or surface are present to highlight significant error induced from model effects, a frictional impact may have generated turbulence in this region. This may be responsible for the elongation presented in Figure 28. The model equation 2.1, an empirical relationship formed from

the collected data, addresses these discrepancies displaying a clear conical shape of velocity in Figure 30, Figure 32 and Figure 34.

One set of samples was collected for a vertical plane through a jet. Another collection of these samples, at a different centreline distance, would present more evidence for the identification of the source of error. In addition, there is also the assumption that the symmetry characteristics presented in this data hold true for all distances from the outflow. However, research conducted increases confidence that this is applicable throughout the length of the velocity field.

The error discussed is considered as relatively inconsequential due to the consistency of the radial velocities recorded for the entire centreline distance, identifiable in Figure 28.

Characteristic Regions of Jet Flow

The velocity field data collected indicates two clear regions of flow which are displayed in Figure 7 and Figure 9. Figure 7 presents the end of the core region of flow at 0.08=D/x, which corresponds to a core region length of 0.325m » 12.5D. However, this is much larger than was anticipated, with the core region length according to Albertson et al. (1950) two times shorter than this at 6.2D. In the experimentation conducted by Albertson et al. (1950) the outflow nozzle was modelled in steel and carefully rounded whereas this project experimentation utilised copper with a straight edge. Generally, steel pipework has thicker walls, compared to that of copper, and the rounded edge suggests that the characteristic outflow is less sharp. The characteristic of sharpness for the outflow nozzle will change the velocity field generated, as the sharper the nozzle the less eddies generated internally. Sharpness will also induce a larger core region. Due to lack of comparative information about the nozzle specification the level of uncertainty is noted.

Albertson et al. (1950) proposed, that there is a change in rate of diffusion at the boundary between transitional and developed flow, however this characteristic is not identifiable from the data. This may be due to measurement resolution of data collected. When Figure 11 is evaluated, the angle of the line of best fit would slightly vary depending on distance from the outflow, particularly evident from data closer to the outflow sitting above the line of best fit. This was supported by characteristic difference in residual variance, eluding to a change in flow experienced. However, this inference is not significant enough to support the theory of Albertson et al. (1950). In addition, Figure 26 presents a visualisation of the data collected where the diffusion rate appears consistent.

Evaluation of formed numerical relationships of decay

Unifying relationships of the data have been determined along the centreline as Equation 1; and radially as Equation 2.1 and 2.2. It was hypothesised that the general form of the centreline equation formed is expected to follow that proposed by Albertson et al. (1950) and that the radial equation would not, therefore the results will be discussed with respect to these hypotheses.

Centreline decay model

Equation 1 is in the general form matching the Albertson et al. (1950) form of equation, giving $\alpha_1 = 0.050$ and $\alpha_2 = 0.906$, which follows the hypothesis.

Statistical analysis provides support for the strength of the linearised form of Equation 1. The strength of the correlation of the linearised relationship between log (x/D) and log (V_x/V_0) was statistically analysed using the PPMC with the output of -0.995. This is an almost perfect negative correlation, particularly significant as this analysis is not resistant to anomalous data due to the squared action within the calculation. Modelling assumptions behind the equation formation were checked through the plot of residuals, Figure 8, which have a constant variation displaying a random scatter about the mean, -0.049, which is very close to 0. This is iterated by the RMS error, 0.0284, a measure of spread of centreline data from Equation 1, which displays very little spread from predicted and measured velocity. The coefficient of determination, R^2, emphasises that 98.96% of the variation of the data is explained by Equation 1. The equation formed is a good fit of the data presented. The correlation, while displaying a strong relationship between variables, does not represent causality. The residual data may withhold an underlying variable of which a trend can't be shown on the residual plot, Figure 8, as it cannot be linearly expressed. However, due to the consistency of this equation formed, which formed grounds for the hypothesis, it is likely that the variables of exit velocity and jet diameter are fundamental in the prediction of velocity at a specific location along the axis, x.

While the equation form shares similarity with the two previous jet prediction formulae from Albertson et al. (1950) and Crushman-Roisin (2019), the comparison of coefficients shows that Equation 1 has smaller values compared to that of previous jet models, see Table 5. When compared graphically in Figure 9, both the Albertson et al. (1950) and Crushman-Roisin (2019) have a very similar decay pattern, with Albertson et al (1950) decay being slightly too rapid compared to the data and Crushman-Roisin (2019) decay slightly too slow. The most significant failing with existing models, however, was not the rate of decay. The length of the core presented by the predictive models was much too small and therefore the change in coefficients of the equations is mainly to transform the graphical curve to the left to account for the larger core flow evident. The discrepancy in characteristic flow regions is unknown; it may be representation of inaccuracies within data, difference in experimental approach or change in experimental conditions. The project is limited by the sample size and more data collection would be required close to the jet outflow in order to more precisely determine where the core region ends, and velocity decay begins.

Table 5: Jet Model Coefficient Comparison

Jet Model	$\boldsymbol{\alpha_1}$	$\boldsymbol{\alpha_2}$
Albertson et al. (1950) *Plain Jet*	0.081	1
Crushman-Rosin (2019) *Submerged Jet*	0.1	1
Equation 1 *Empirical relationship*	0.05	0.906

Propeller models, not mentioned in this section above, display an even shorter core region of flow still. However, this was anticipated due to the propeller immediately inputting a large amount of turbulence that is not present in the jet. Therefore, the processes of velocity field generation are different from the outset.

Radial decay model

Equation 2.1 and Equation 2.2 are not in the general form produced by Albertson et al. (1950), which follows the hypothesis.

The general form was changed from: $V_{x,r} = V_x \exp\left(-\frac{1}{2\alpha_3{}^2}\frac{r^2}{x^2}\right)$ to the form $V_{x,r} = V_x \exp\left(-\frac{1}{2\alpha_3{}^2}\frac{r^2}{x}\right)$ which was generated empirically by experimental data from the physical modelling undertaken this project. The equation represents a very strong negative correlation, statistically analysed using the PPMC for the linearised relationship between log (x/D) and log ($V_{x,r}/V_x$) giving an output of -0.915. The coefficient of determination, R^2, emphasises that 84.73% of the variation of the data is explained by Equation 2.1.

All of the data indicates a strong correlation between the variables. However, upon plotting the residuals graphically, Figure 12, heteroskedasticity is present. This is a modelling assumption check and the non-constant variance displays the equation is ill-defined. Therefore, inferred conclusions from the equations which support the hypothesis are limited. Constant residual variance is restored when data before x = 1 m (displayed by circles), and after 1 m (displayed by crosses) is evaluated independently, as shown by Figure 12. Equation 2.1 is considered limited, despite the constant variation of residuals after x=1m, because a skew of data within the plot of remaining residuals is evident. It should also be noted that only 2 or 3 radial measurements were carried out for each distance of x considered, which is a relatively small representation of the radial flow characteristic. A large confidence in the relationship given in Equation 2.1 is not induced. The region the Equation 2.1 represents is not the most critical region for the application of scour design; with coastal berthing structures being much shallower than 43m, represented by x=1m in the physical model.

A separate equation was determined to represent flow for when x < 1 m, Equation 2.2. This equation enabled the variation of residuals from the model to be more constant, and it is prudent to note that the equation retains the same form with only an altered coefficient. The strength of the correlation of the linearised relationship between log (x/D) and log ($V_{x,r}/V_x$) was statistically analysed using the PPMC with the output of -0.945. This is a very strong negative correlation, stronger than that of Equation 2.1. The coefficient of determination, R^2, details that 95.83% of the variation of the data is explained by Equation 2.2, over 10% more explanatory than when the entire measured jet axis is considered. The equation presents a good correlation between the variables. A comparative plot of the residuals where x<1m for equation 2.1 and 2.2 is shown in Figure 14, the variance of the data is reduced, shown by crosses, however there is considerable skew which displays modelling assumptions made have not been met.

In some places the model Equation 2.1 doesn't fit the collected data quite as well, see Figure 29, where the centreline distance from the jet is 1.5m but can also be evidenced on other figures of varying distance. Experimental procedures have the most uncertain measurements taken are where turbulence is evident. It is likely that particularly in the latter part of the flow, the number of samples averaged was not great enough to average out the impact of turbulence. Despite this, the scatter from the curve in Figure 28 is still fairly evenly distributed and the data appears to be well represented. This is supported by Equation 2.1 presenting a jet flow while other models predicted minimal velocity incursions shown in Figure 16 to Figure 25.

The jet radial model equations, Albertson et al. (1950) and Crushman-Roisin (2019), badly represent the radial decay of velocity at all transects measured. It is highlighted in Figure 15 that the radial flow prediction holds more error the closer to the outflow it gets in an exponential way. This indicates that an underlying variable in the prediction of radial velocities is at play which is amplified by requiring an accurate centreline velocity to inform the radial velocity anticipated. Since the centreline prediction of the jet models decay too rapidly, due to a shorter characteristic flow, more error was anticipated closer to the jet outflow.

Statistical confidence is prevalent in the both Equation 2.1 and 2.2 from the data collected for the proposed radial model, explaining 84.73% (for the length of the velocity field) and 95.83% (for $x < 1$ m) respectively. The equations also display the least RMS error in total radially, as identified in Table 4. Therefore, despite limitations the equations formed are better than existing jet models at predicting the flow velocity field generated in this physical model. Greater resolution of the radial data collected would enable trends to be more easily identified which could improve upon this equation.

Evaluation of the validity of propeller models

The hypothesis, that the propeller models would be less accurate in the prediction of the jet velocity flow field, was met through comparative data analysis of experimental data collected in this project.

A visual comparison of the velocity flow fields anticipated for each model based on the diameter of the outflow and exit velocity is visually presented from Figure 36 to Figure 41. The characteristic difference in the flow fields predicted by the jet and propeller models is fairly obvious with the shorter core region of flow. Numerical comparison of RMS error for each model is summarised centrally, radially and combined in Table 6. It indicates than ten times the RMS error is exhibited from the use of propeller model than the empirical formulae formed. In comparison of existing models, jet models can be seen to always exhibit less error than that of a propeller equation. The best propeller model has 1.4 times more error than Albertson et al. (1950). Therefore, in the design of scour protection subject to jet mooring, agreement is made with Verheij & Stolker (2007) that propeller prediction design formulae are not adequate.

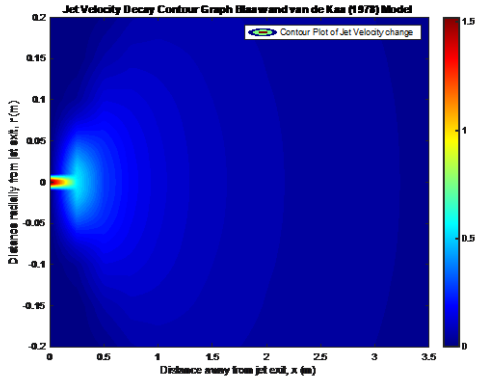

Figure 36: Velocity Profile of Propeller Model from Blaaw and van de Kaa (1978)

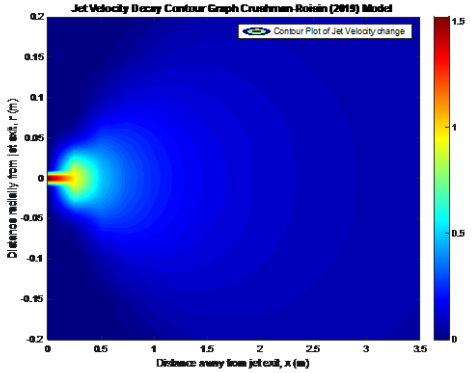

Figure 37: Velocity Profile of Jet Model from Cushman-Roisin (2019)

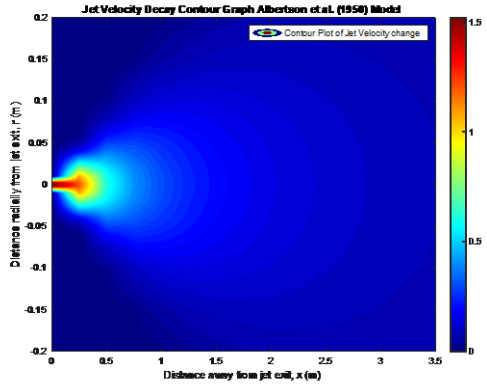

Figure 38: Velocity Profile of Jet Model from Albertson et al. (1950)

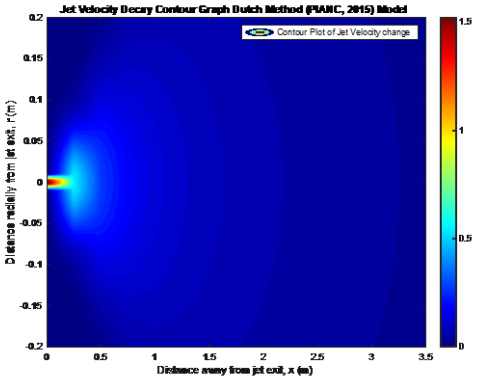

Figure 39: Velocity Profile of Propeller Model from The Dutch Method (PIANC,2015)

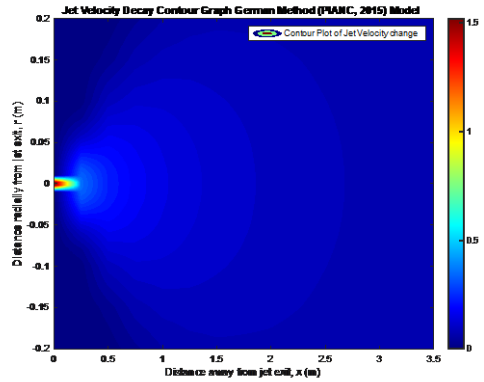

Figure 40: Velocity Profile of Propeller Model from The German Method (PIANC,2015)

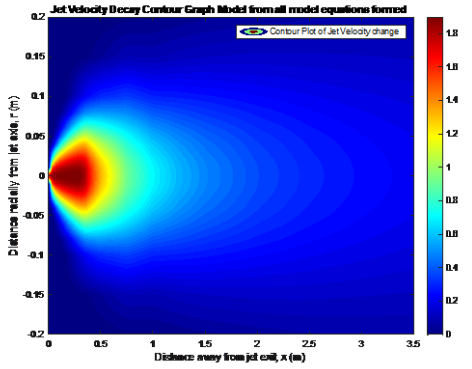

Figure 41: Velocity Profile of Empirical Model Formed from Eq. 1 at centreline, Eq2.2 radially x<1m, otherwise radially Eq.2.1

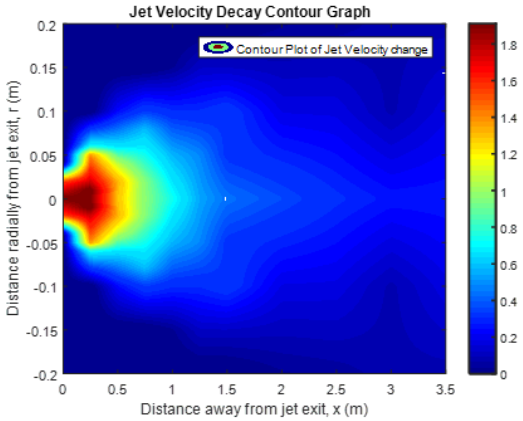

Figure 42: Velocity Profile of data collected

Table 6: Summary of Model Errors

Model	Centreline RMS Error	Radial RMS Error	Combined Centreline and Radial RMS Error (Averaged)
Equations 1, 2.1 and 2.2, *Empirical jet*	0.0284	0.0598	0.0441
Equations 1 and 2.1, *Empirical jet*	0.0284	0.0820	0.0552
Albertson et al. (1950), *Plain Jet*	0.3935	0.4417	0.4176
Crushman-Rosin (2019), *Submerged Jet*	0.4752	0.4621	0.4687
Dutch Method (PIANC, 2015), *Propeller*	0.6335	0.5477	0.5906
Blaauw & van de Kaa (1987), *Propeller*	*0.6349*	0.5708	0.6029
German Method (PIANC, 2015), *Propeller*	0.6720	0.6212	0.6466
Berger et al. (1981), *Propeller*	0.6032	-	-
Hamill (1987), *Propeller*	0.6546	-	-

Implications of Research for Industry

When the physical model is scaled back up to the prototype, the implications on scour design can be realised. The prototype specifications and model scaling are given in the methodology.

The exit velocity in this experiment was 12.7m/s, closely following the scaling previously specified based from the Solano Ferry. This ferry features a typical catamaran hull with length 41.30m and maximum draft of 1.5m (Hamilton Jet., 2020). According to berthing design guidance PIANC (2016) the dredging depth is a simple calculation as shown below; an illustrated diagram of the components making up a determined dredge depth is also provided by Thoreson (2018), given below.

$$Dredge\ Depth\ (m) = 0.9m\ Underkeel\ Clearance + y\%\ of\ Vessel\ Draft$$

Where:

y= 10% of draft in sheltered conditions;

y= 30% where wave height is up to 1m;

y= 50% where wave heights are greater than this.

Considering the dredge depth design guidance above, the Solano Ferry berth would require a dredge depth of only 1.05m to 1.65m depending on conditions. The scaled-up core region of the jet is 13.98m in length which means that the exit velocity of the water jet, when deflected to the seabed, will not have decayed. Water velocities of 12.7m/s at the bed of the berth, from the jet flow centreline, should be anticipated. Even when the ferry is not the design vessel, 14m of dredged depth is not shallow. Therefore, for scour protection design, the decay equations will be less helpful than the characteristic core region length since dredged berths, deeper than 14m for ferries, is unlikely.

These findings also reveal the probable development in scour protection design approach. Utilisation of existing equations converting water velocities to quantified rock armour protection would be sized much too large to be practical. Therefore, the speculation is made that the use of concrete mattresses will increase over the coming years, to allow for thinner protection, as the use of water jet propulsion vessels increase.

Recommendations for Future Work

While the research into water jets was fuelled by Coastal Engineering application of scour, the understanding of water jets is applicable to many areas such as offset jets within drainage systems, slot fishways and hydraulic engineering (Zhou, Zhang, Li, & Xu, 2018). Therefore, further work could escalate in a multitude of directions. It is hoped that this project has added to the research within scour caused by water jets and that this project could inspire further research. More specific recommendations of further work are given below.

Improving Instrumentation

If the experimentation was to be undertaken again there are a number of changes that would be made in order to ensure a data set with a higher resolution was collected. This would enable more confidence in the statistical significance of data analysis.

The Acoustic Doppler Velocimeter (ADV) would enable directional velocities to be collected at a rate of 64Hz, enabling analysis into the vortices present within the flow. However, there are a number of challenges as discussed in Appendix C surrounding the still basin and positively buoyant seeding. A solution could involve a dual-basin, where the water jet is submerged in turbulent water with lots of suspended sediment and a pipe connects the pump to the outflow within a still basin. This would enable the suspension of sediments while still controlling the conditions impacting on the flow characteristics.

Aims of Research

This investigation into jet hydrodynamics has highlighted the uncertainty of the use and accuracy prediction formulae available to engineers, namely that the core region of the jet has yet to be accurately parametrised. Flows from water jets take longer to decay than propeller models, due to the absence of turbulence formed from rotational flow. Future work surrounding the parametrisation of factors which impact this core region of flow would enable the increase in the accuracy of prediction models and design applications. However, in order to achieve this, data gaps within research, as discussed in Section **Error! Reference source not found.**, are prevalent and therefore a more comprehensive set of experimental studies changing minor aspects of the experiment, such as orifice shape and vessel characteristics, would need to be assessed first. In addition, previous research would become contextualised and easily compared as experimental set up could be quantitatively removed.

Another major uncertain element of water jet flow mooring is the impact that the water jet reflection from a bucket differs from that of the unconfined flow investigated. A change in the characteristic flow shape and decay is critical to ensure methods to predict the velocity induced are reliable ensuring safe and economical design of scour protection.

Conclusion

The findings of this project contribute significantly to coastal engineering. Since jet propulsion is a new consideration for the design scour protection within marinas and harbours, existing research is limited. The comparison of the existing models to collected data and the generation of new empirical models indicates the need for further research but many conclusions have been made.

Characteristics of Flow

The investigation into the characteristics specific to jet flows have been concluded to be symmetrical, similarly to propeller induced flows but at different dispersion rates. The circular outflow produces a velocity field characterised by circular symmetrical cross section of flow with a conical side profile, but it remains unknown what characteristic would prevail with a different jet nozzle shape. The velocity field data

indicated two clear regions of flow; the core region and the established flow region ($V_x<V_0$). The core region identified from data collected is larger than any existing jet model accounted for, parametrised at 12.5D from the nozzle. In line with previous research turbulence is prevalent in the jet velocity field and accounts for the small errors within the data. The turbulence encountered is most significant at the boundaries and in the latter stages of flow, much reduced from that of propeller induced flows.

Numerical Relationships

Unifying the data collected into an empirical model has allowed identification of statistically significant data for; centreline velocity flow between log(x/D) and log (V_x/V_0) and radial velocity flow between log (x/D) and log ($V_{x,r}/V_x$). Three equations were formed as part of this project, Equation 1 for the centreline of flow when $V_x<V_0$, Equation 2.1 for radial flow based on all radial transect data and Equation 2.2 for $x <$ 1 m for radial flow. In order to minimise error, the equations should be used as follows; Equation 1 for the centreline of flow, Equation 2.1 for $x \geq 1$ m for radial flow and Equation 2.2 for $x < 1$ m for radial flow.

The hypotheses that the general forms of the equation through the centreline and radially would follow the work of Albertson et al. (1950) was fully met. The centreline equation formed followed the general form and the radial data did not follow the gaussian distribution. In addition, the empirical model formed in this project has the least RMS error both centrally and radially when the data is compared to the existing models. Furthermore, the hypothesis that the propeller models would not adequately predict the velocity field induced by a jet was met, holding the highest RMS errors in all cases.

Implications on scour design

While velocity decay equations throughout the velocity field have been established in this project, the biggest implication for the coastal engineering industry is the length of the characteristic core region of jet flow, 12.5D. Typical ferries, such as the Solano Ferry, have a core region of flow, scaled-up from the physical model, of 13.98m. For the berthing utilised by the Solano Ferry (with dredge depth of less than or equal to 14m), the exit velocity of the jet deflected to the seabed will not have decayed. Scour protection is required to prevent undermining of berthing structures like quay walls. Existing models underestimate the length of the core region which will greatly impact on the jet flows predicted.

In conclusion, this project has demonstrated that coastal engineers need to be aware of the characteristics and behaviour of jet propulsion systems rather than relying upon existing models to calculate safe scour protection. This is an area that will only continue to grow over the coming years therefore more research should be undertaken in this area to gain confidence in the safety of design.

Acknowledgements

My sincerest gratitude to Dr Jon Miles who supported me throughout this project development and all other University of Plymouth staff who helped to envisage the physical model set-up and made it a reality. I also want to thank my friends and family for their support in this work and everyone who guided me through the editing

process. It has been a pleasure to work on a paper of which has great interest to me, within an area very relevant in coastal engineering and tackling a real contemporary issue faced in industry.

Nomenclature

α	Coefficient of Velocity Decay (-)
β	Blade Area Ratio (-)
A	Outflow opening area $= \frac{\pi D^2}{4}$ (m^2)
Ct	Thrust Coefficient (-)
D	Diameter of Jet Outflow (m)
h	Height of jet above sea bed (m)
P’	Pitch Ratio (-)
r	Radial Distance from Jet Centreline (m)
r_C	Pearson’s Product Moment Correlation Coefficient (-)
V_0	Exit Velocity (m/s)
V_x	(Predicted) Max Time Average Velocity at position x along the jet axis (m/s)
$V_{x,r}$	(Predicted) Max Time Average Velocity at distance ‘x’ along the jet axis and distance ‘r’ radially from the jet axis (m/s)
x	Distance along the Jet Centreline (m)

References

Albertson, M., Dai, Y., Jenson, R., & Rouse, H. (1950). Diffusion of Submerged Jets. American Society of Civil Engineers, Paper No. 2409.

Berger, W., Felkel, K., Hager, M., Oebius, H., & Schale, E. (1981). Courant provoque par les berges et solution pour eviter l'erosion du lit du haut rhin. 25th Congress. Edinburgh: PIANC.

Blaauw , H., & van de Kaa, E. (1987). Erosion of bottom and sloping banks caused by the screw race of manoeuvering ships. Antwerp: 7th International Harbour Congress.

Crushman-Roisin, B. (2019). Chapter 9: Turbulent Jets. In B. Crushman-Roisin, Environmental Fluid Mechanics.

Hamill, G. (1987). Characteristics of the screw wash of a manoevering ship and the resulting bed scour. Ph.D. Thesis, Queen's University of Belfast.

Hamill, L. (2011). Understanding Hydraulics. Baisingstoke: Palgrave.

Hamilton Jet. (2019). WaterJet Overview. Retrieved October 2019, from HamiltonJet: https://www.hamiltonjet.com/global/waterjet-overview

Hamilton Jet. (2020). Fast Ferries around the Globe. Retrieved April 2020, from https://www.hamiltonjet.com/global/type/fast-ferry

Hawkswood, M., Evans, G., & Hawkswood, G. (2015). Berth Scour Protection For Fast Ferry Jets. ICE Publishing.

Hoffmans, G., & Verheij, H. (2011). Jet Scour. Maritime Engineering, 164(4).

Lam, W.-H., Song, Y., Raghunathan, S., Hamill, G., & Robinson, D. (2011). Investigation of a ship's propeller jet using momentum decay and energy decay. Canadian Journal of Civil Engineering, 38(6), 605-615.

Li, K., & Li, W. (2013). Study on the Acceleration Process of Water-jet Propulsion Ship. Applied Mechanics and Materials, 263-266, 756-761.

Núñez-González, F., Koll, K., & Spitzer, D. (2018). Experimental study of the velocity field induced by a propeller jet in an inland-ship model and the related bed scour. River Flow.

Núñez-Gonzalwz, F., Koll, K., Spitzer, D., & Söhgen, B. (2017). Scour Geometry and flow velocities induced by experimental ship propeller jet. River Sedimentation, 1229-1236.

Nyantekyi-Kawakye, B., Clark, S., Tachie, M., Malenchak, J., & Muluye, G. (2015). Flow Characteristics within the recirculation region of three-dimensional turbulent offset jet. Journal of Hydraulic Research, 53(2), 230-242.

PIANC. (2015). WG180 Guidelines for Protecting Berthing Structures from Scour Caused by Ships. Maritime Navigication Commission.

PIANC. (2016). Report n 149/Part II: Guidelines for Marina Design. Maritime Navigation Commuission.

Quinn, W., & Militzer, J. (1989). Effects of nonparallel exit flow on round turbulent free jets. International Journal of Heat and Fluid Flow, 139-145.

Stirling, W. (2013). World's biggest yavht has the power of large wind farm. Retrieved September 2019, from The manufacturer: https://www.themanufacturer.com/articles/worlds-biggest-yacht-has-the-power-of-large-wind-farm/

Sumer, B., & Fredsøe, J. (2002). The Mechanics of Scour in the Marine Environment. World Scientific, 17.

Thoresen, C. (2018). Port Designer's Handbook (Vol. 4th Edition). ICE Publishing.

U.S. Army Corps of Engineers. (2011). Coastal Engineering Manual. Washing, D.C.: U.S. Army Corps of Engineers.

Valeport. (2020). Retrieved April 2020, from https://www.valeport.co.uk/content/uploads/2020/04/Model-001-002-Flow-Meter-Datasheet-April-2020.pdf

Verheij, H. (1983). The Stability of bottom and banks subjected to the velocitites in the propeller jet behind ships. 8th International Harbour Congress. Antwerp.

Verheij, H., & Stolker, J. (2007). Hydro jets of fast ferries require proper designed quay walls. 2nd International Maritime-Port Technology Conference. Singapore.

Whitehouse, R., Sumer, B., & Tørum, A. (2001). Scour around coastal structures: a summary of recent research. Coastal Engineering, 44(2), 153-190.

Zhou, M., Zhang, J., Li, X., & Xu, W. (2018). Numerical Study of the Velocity Decay of Offset Jet in a Narrow and Deep Pool. Water.